Emad Oveisi

Scanning and Analytical Transmission Electron Microscopy

Introduction to STEM

MSE-735

Summer 2023

Emad Oveisi

Contents

Emad Oveisi

Types of transmission electron microscopes

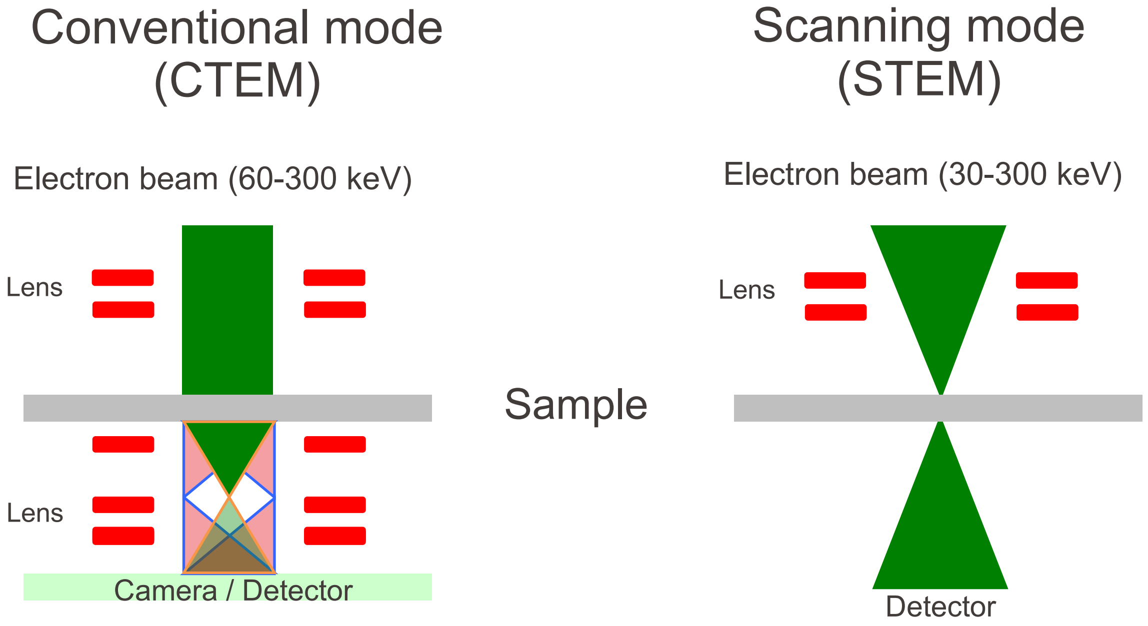

The most important lens:
Objective lens

The most important lens:
Condenser lens

Principles of STEM

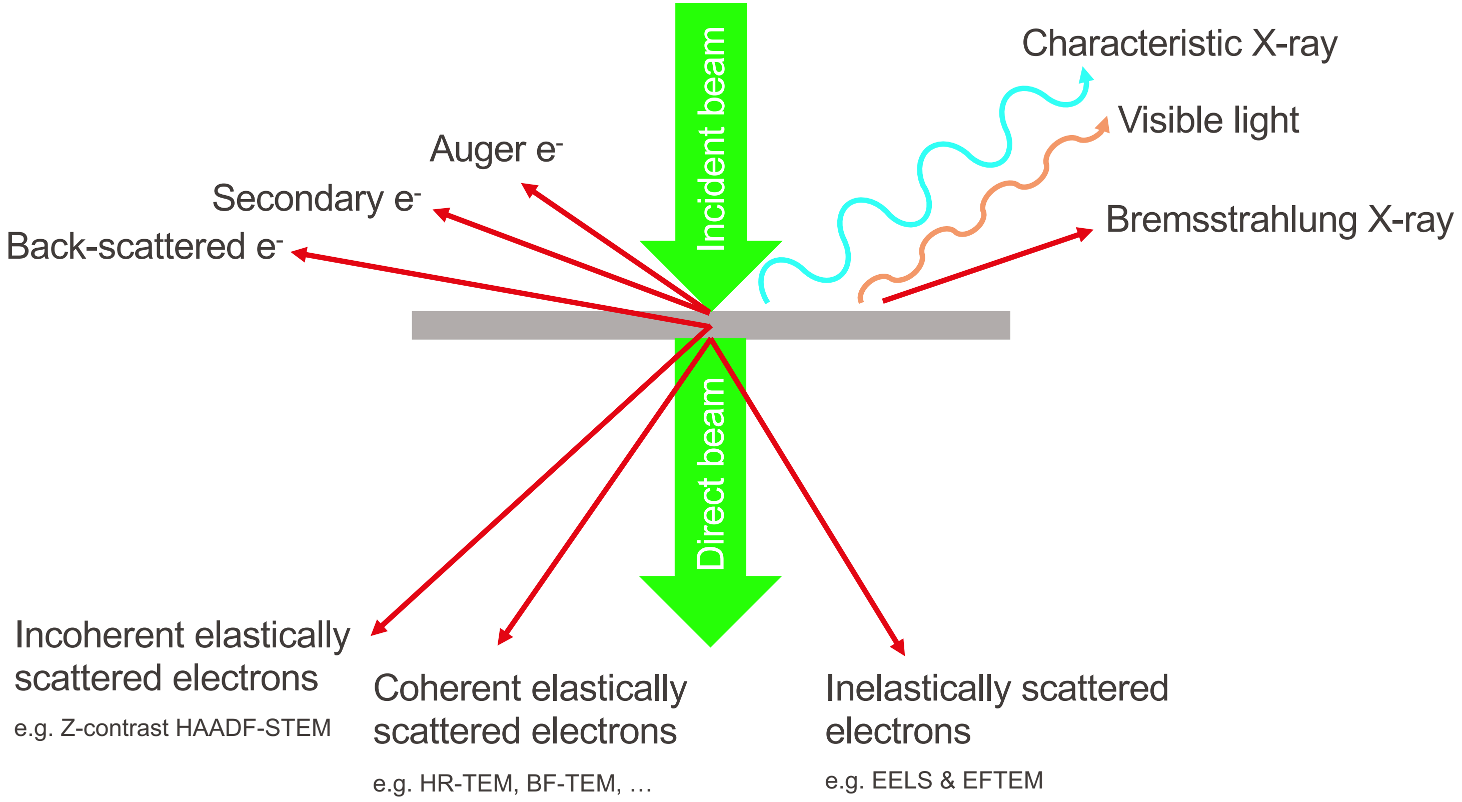

Emad Oveisi

Principles of STEM

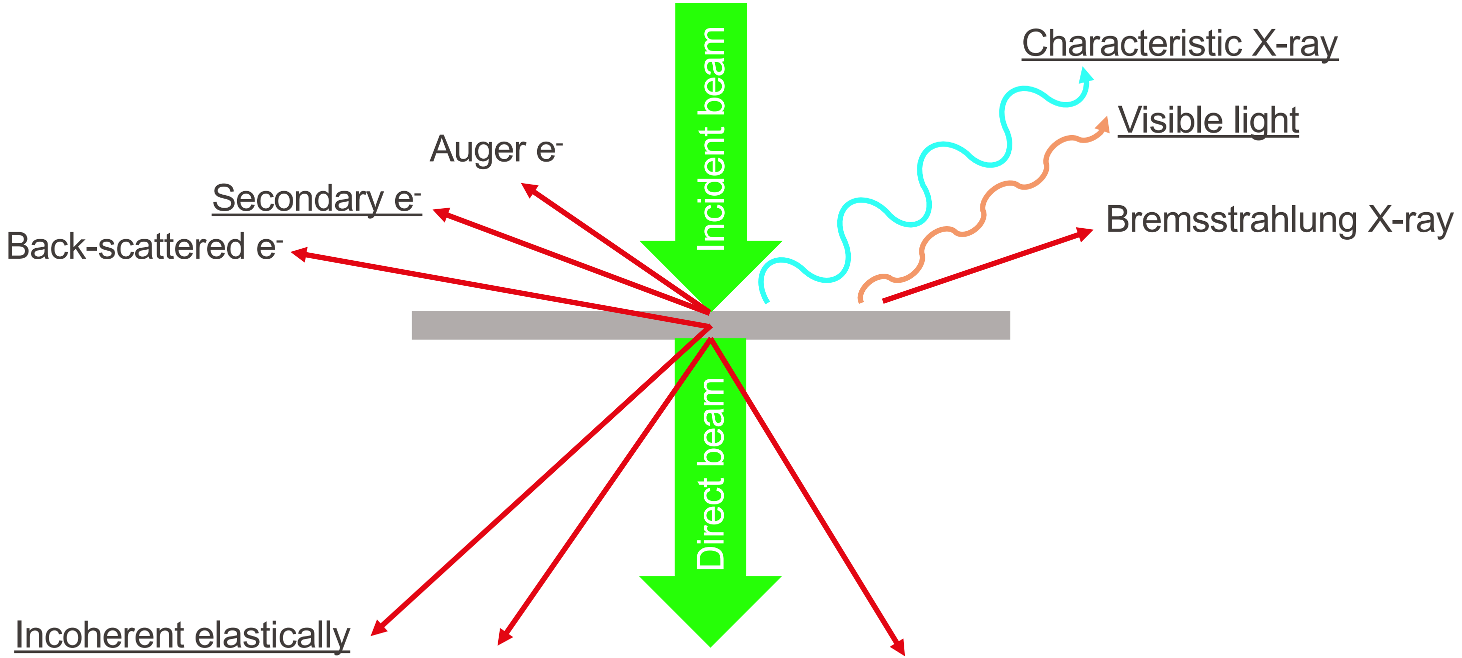

Incoherent elastically scattered electrons

e.g. Z-contrast HAADF-STEM

Coherent elastically scattered electrons

e.g. HR-TEM, BF-TEM, …

Inelastically scattered electrons

e.g. EELS & EFTEM

Principles of STEM

In STEM the electron beam is focused to a fine spot which is then scanned over the sample in a raster. This is similar to how scanning electron microscopy works.

By rastering the beam across the sample, STEM is suitable for analytical spectrum imaging techniques such as EDX and EELS.

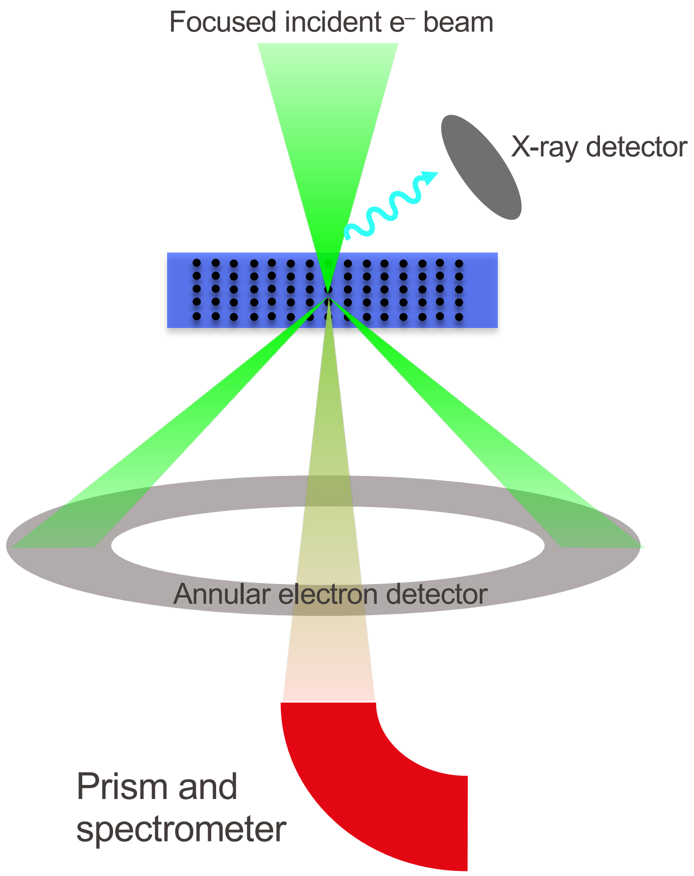

Principles of STEM

Electromagnetic lens focuses electrons from FEG on to the sample (Condenser systems)

Beam deflectors scan beam across the sample

For each probe position (x,y) record on:

- Detector: Signal intensity $I_{(x,y)}$ → Image
- Spectrometer: Integrated signal from hyperspectral datasets → 3D data-cube (e.g. EELS and EDX spectrum image)

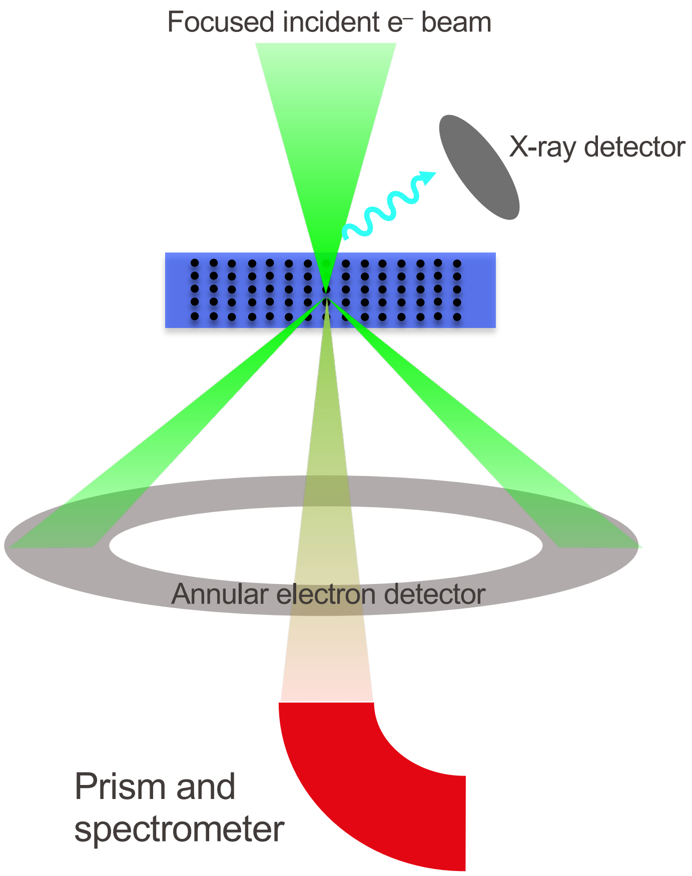

Emad Oveisi

Principles of STEM | Magnification and scanning

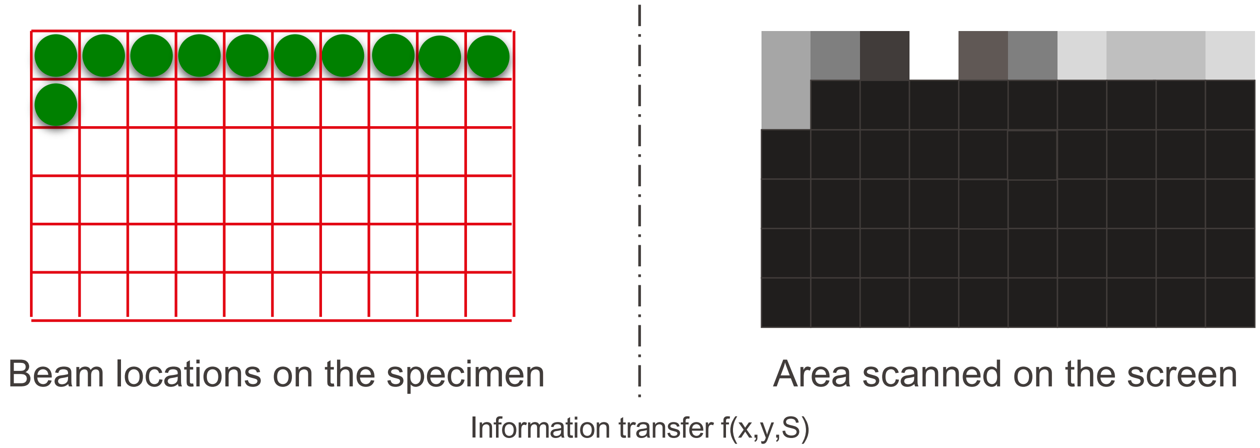

- Image formed by recording the time sequence of intensities for any particular small portion of diffraction pattern as the incident beam is scanned over the sample (using pair of deflector or scan coils)
- Monitor and scanning coils are synchronized
- Intensity of each pixel is proportional to signal collected by the detector
- When changing the magnification, we just change the raster size (no change in optics)

Magnification = Image size (e.g. display) / Raster size on the specimen

Principles of STEM | Magnification and scanning

All the STEM images appear on the computer screen at a magnification that is controlled by the **scan dimensions** on the specimen, not the lenses of the microscope.

This is a fundamental difference between scanning and static image formation.

Magnification = Size of the screen / Raster size on the sample

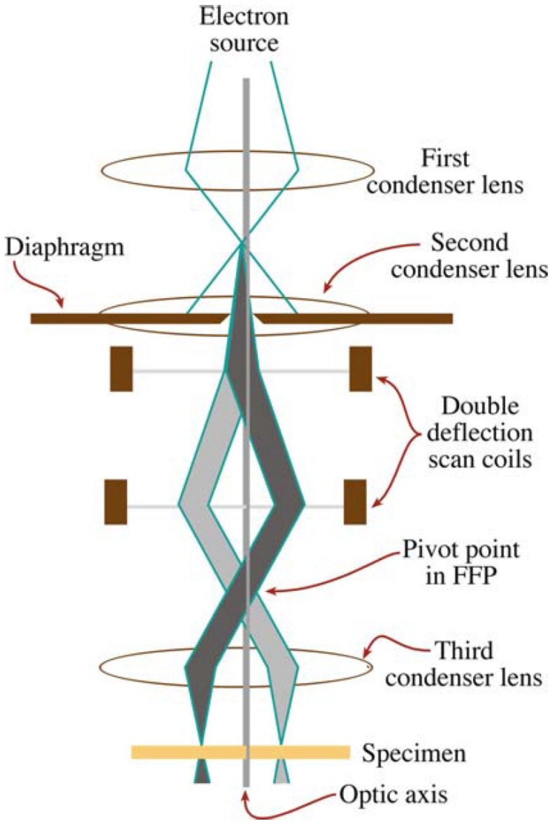

Principles of STEM | Magnification and scanning

Emad Oveisi

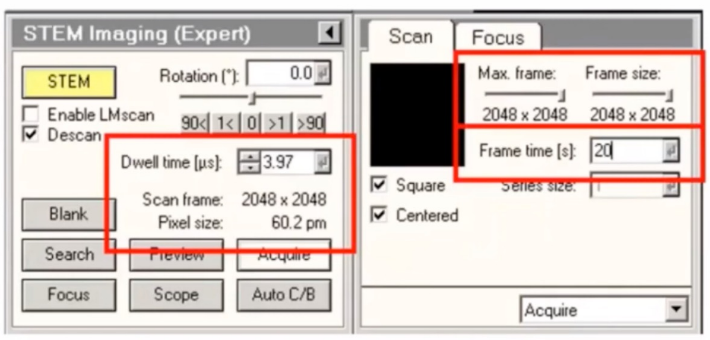

Scan frame x Dwell time = Frame time

e.g. 2048x2048 x 3.97 usec = 20 Sec

If for Mag. = 640 kx, the Pixel size is 60.2 pm, for Mag. = 2.55 Mx calculate:

a) The pixel size,

b) Scan area, and

c) Size of the screen

Probe forming | 2-condensor lens system

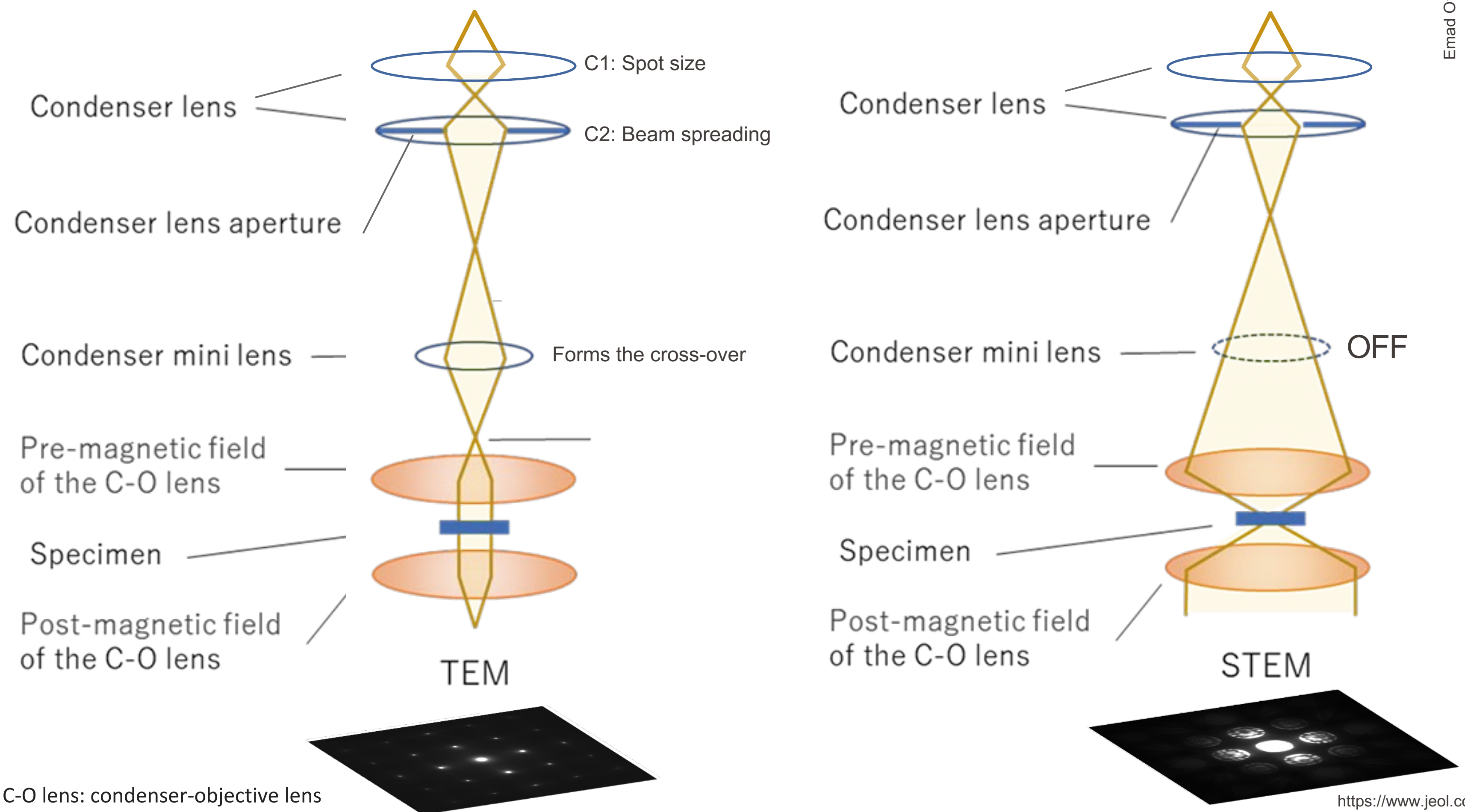

C-O lens: condenser-objective lens

https://www.jeol.com/

Probe forming

Consider exact 2-beam condition:

Imagine a convergent beam, not fully focused on sample
→ Decompose as parallel rays of different directions

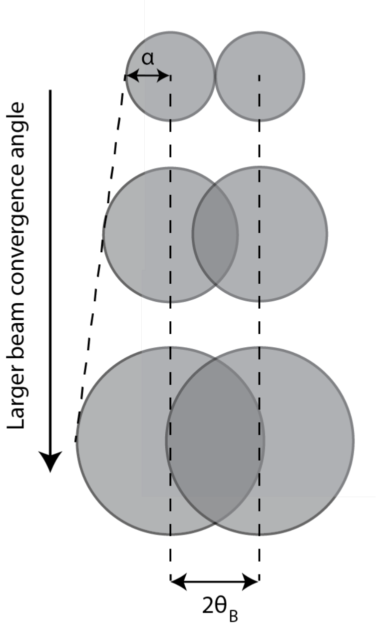

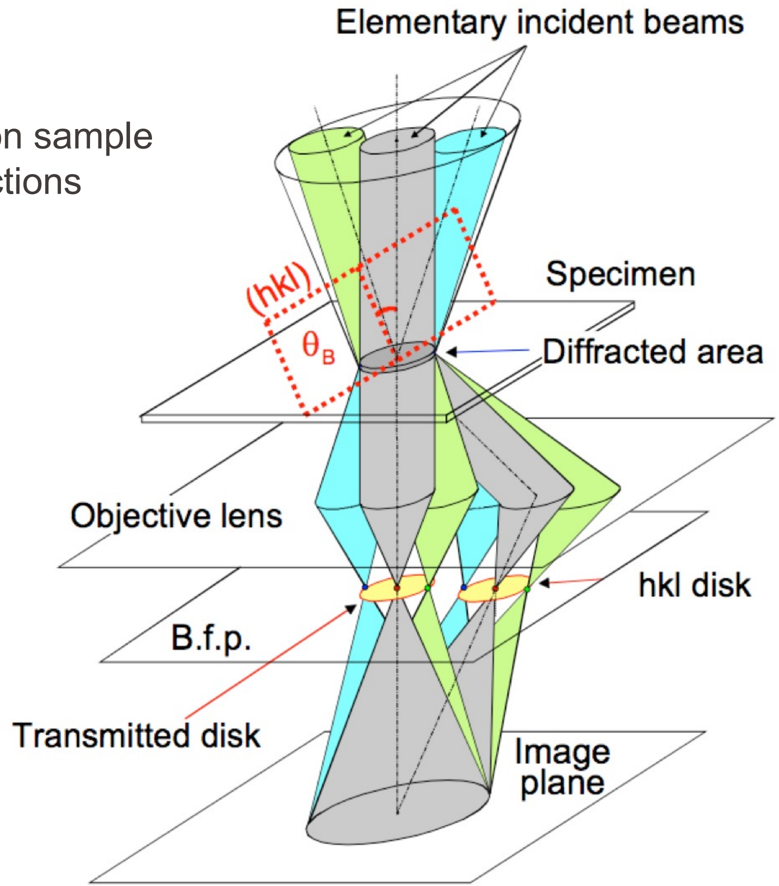

Figures by Jean-Paul Morniroli

Probe forming

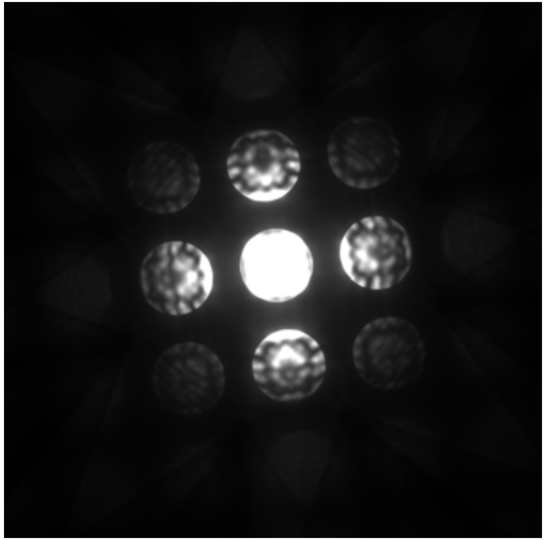

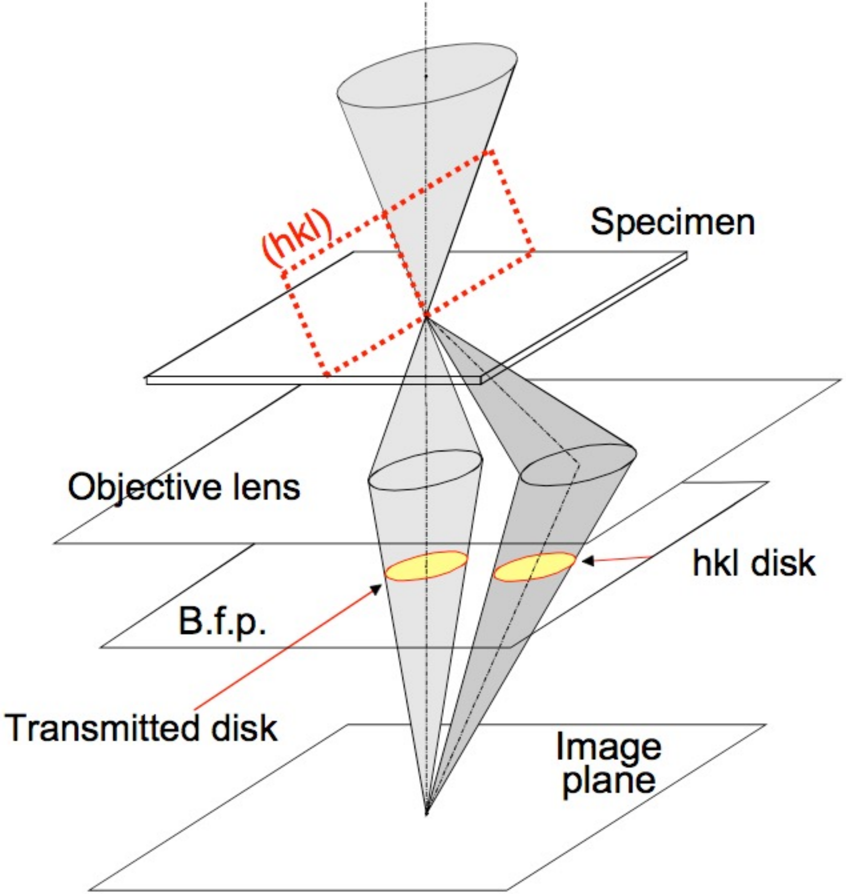

Probe forming | 3-condensor lens system

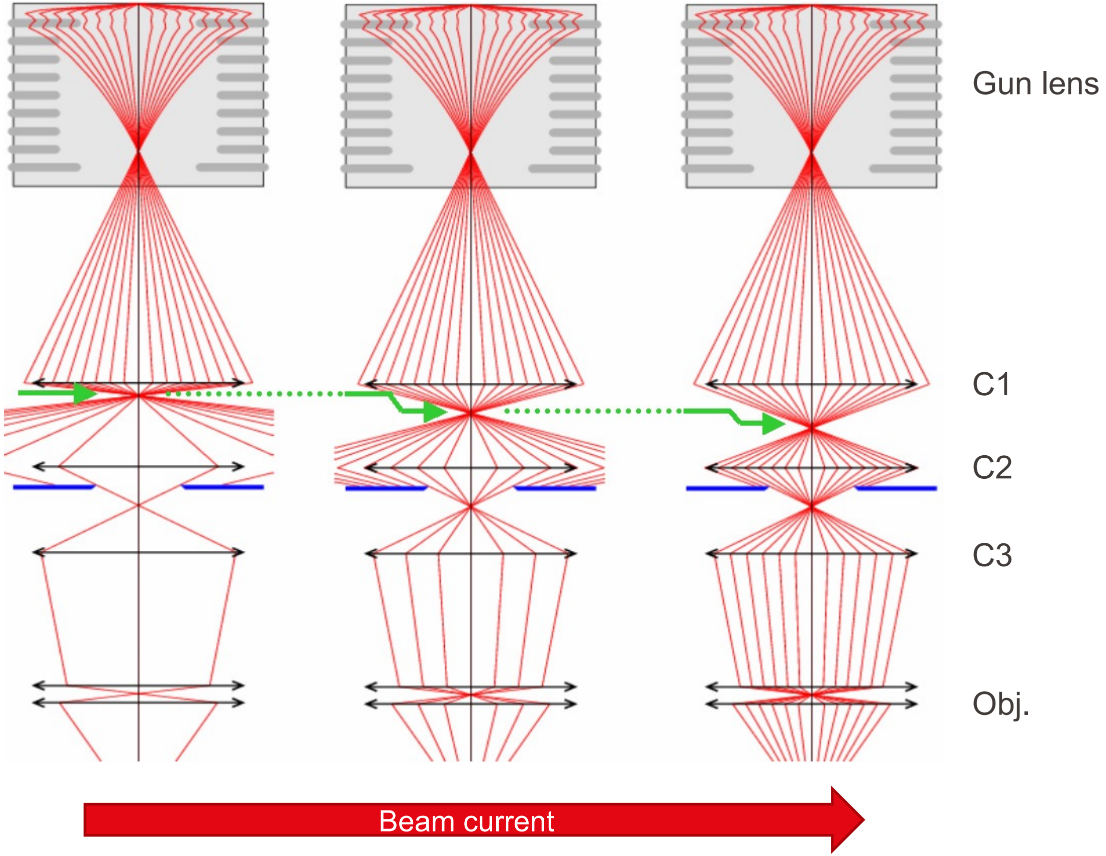

Probe forming | 3-condensor lens system

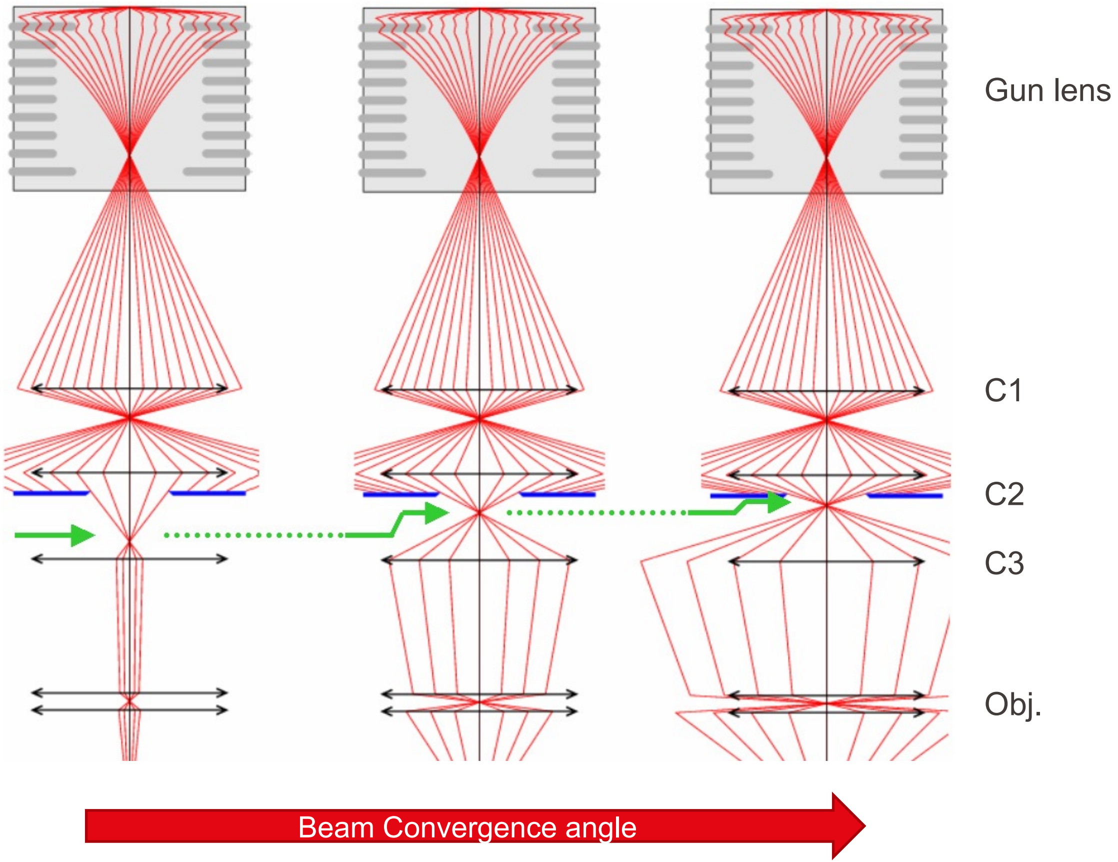

Aberrations

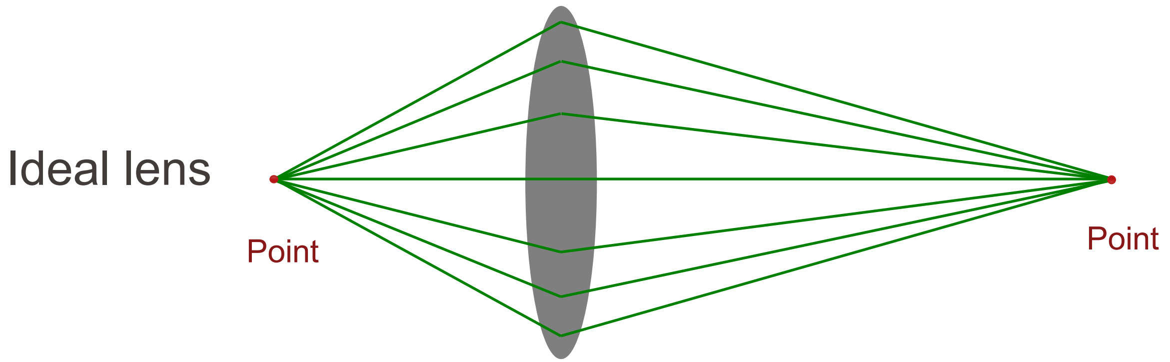

A point source is focused to a point

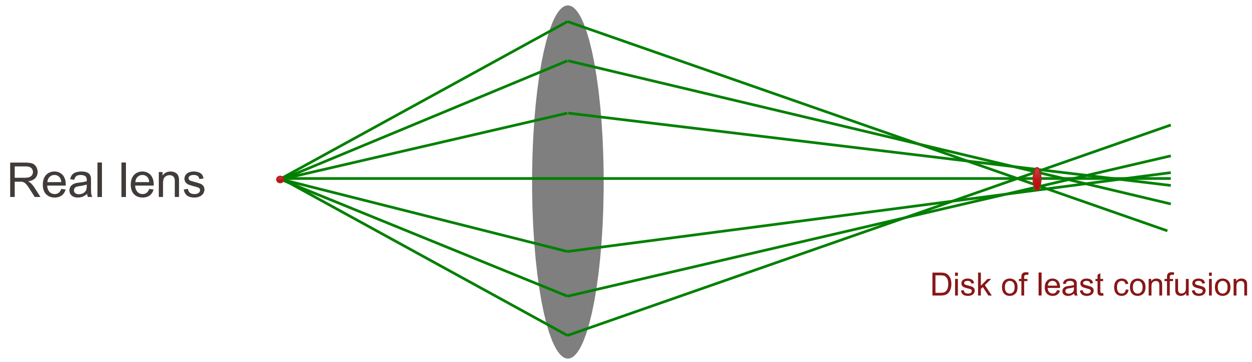

A point source is focused to a disk

Lens aberrations limits resolution!

Aberrations

- **Lens aberrations**
  - Chromatic aberration
  - Spherical aberration
  - Astigmatism

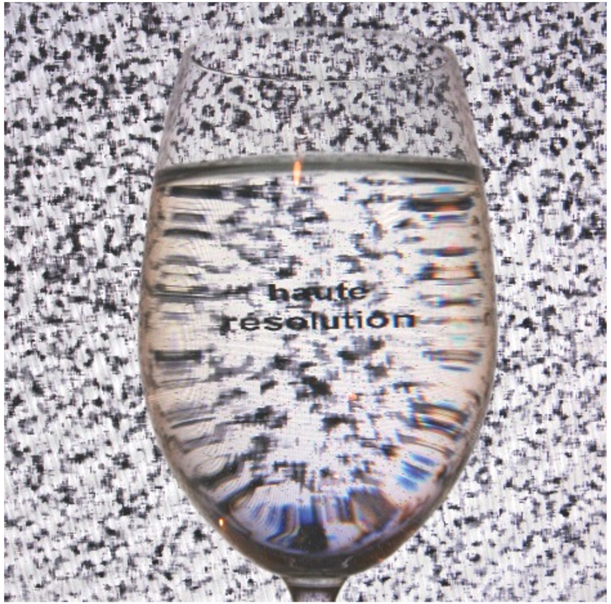

Diffraction effect (aperture limit)

STEM resolution is detemined by the size of the probe and stability of the instrument

Resolution in HR-S/TEM limited by aberrations, especially Cs

Aberrations

- Chromatic aberration (Cc)

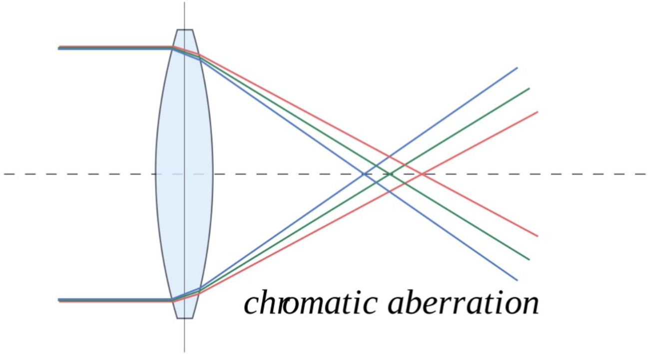

- Lens cannot focus all energies to the same convergence point.
- Electrons of lower energy will be bent more strongly.
- Correcting the aberration is necessary, otherwise the resulting image would be blurry and delocalized, a form of aberration where periodic structures appear to extend beyond their physical boundaries.
- Cc increases with source energy spread.

Aberrations

Emad Oveisi

- Spherical aberration (Cs)

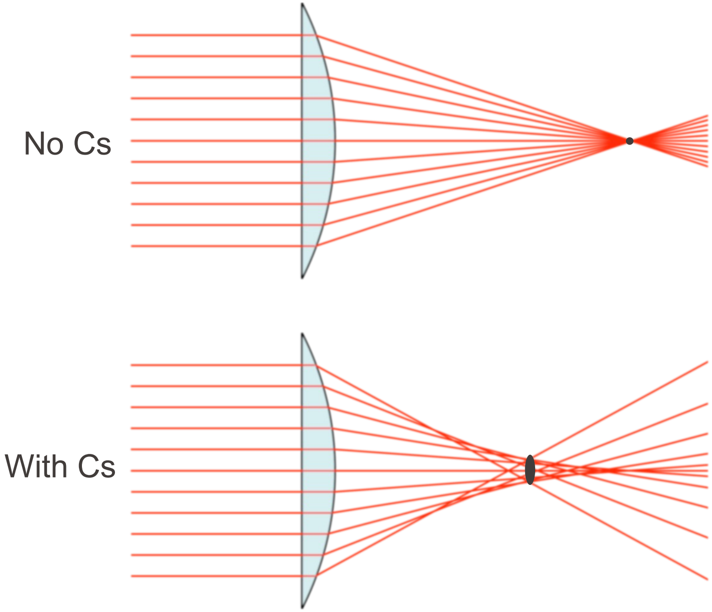

- Parallel rays that pass through the central region of the lens focus farther away than the rays that pass through the edges of the lens.
- Results in multiple focal points and thus a blurred image.
- Larger probe and lower resolution.

Core of the galaxy M100 ©NASA

Aberrations

- Spherical aberration (Cs)

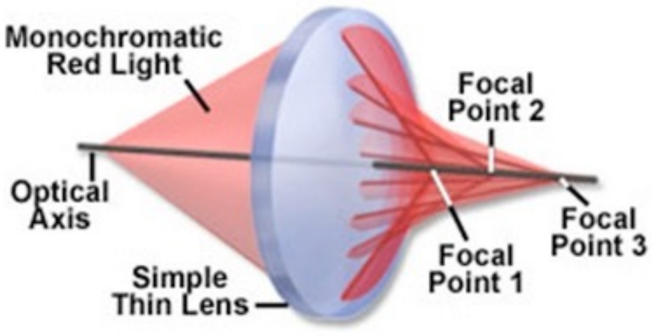

$$\alpha_{opt} = \left(\frac{4\lambda}{C_s}\right)^{\frac{1}{4}}$$

$$d_{opt} = 0.61 \frac{\lambda}{\alpha_{opt}} = 0.43\, \lambda^{\frac{3}{4}} C_s^{\frac{1}{4}}$$

- Focal length depends on the distance from optical axis
- Image of the object is dispersed along the optical axis

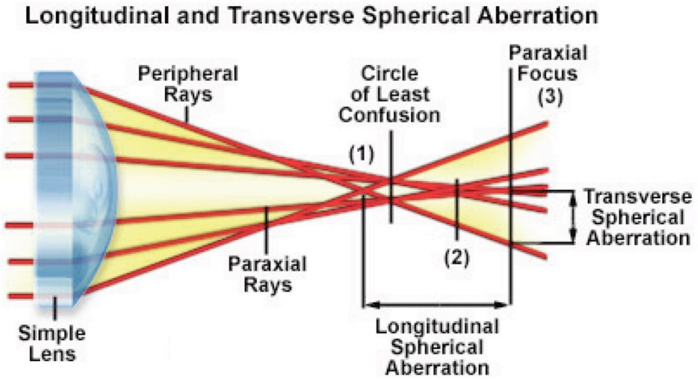

Aberrations

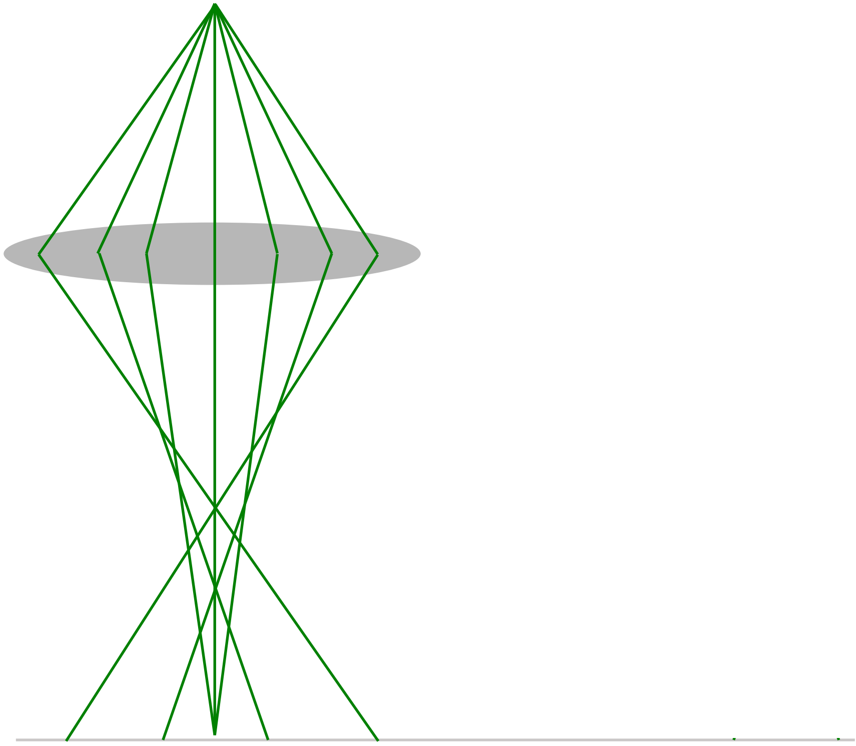

How to lower the effect of spherical aberration?

Aberrations

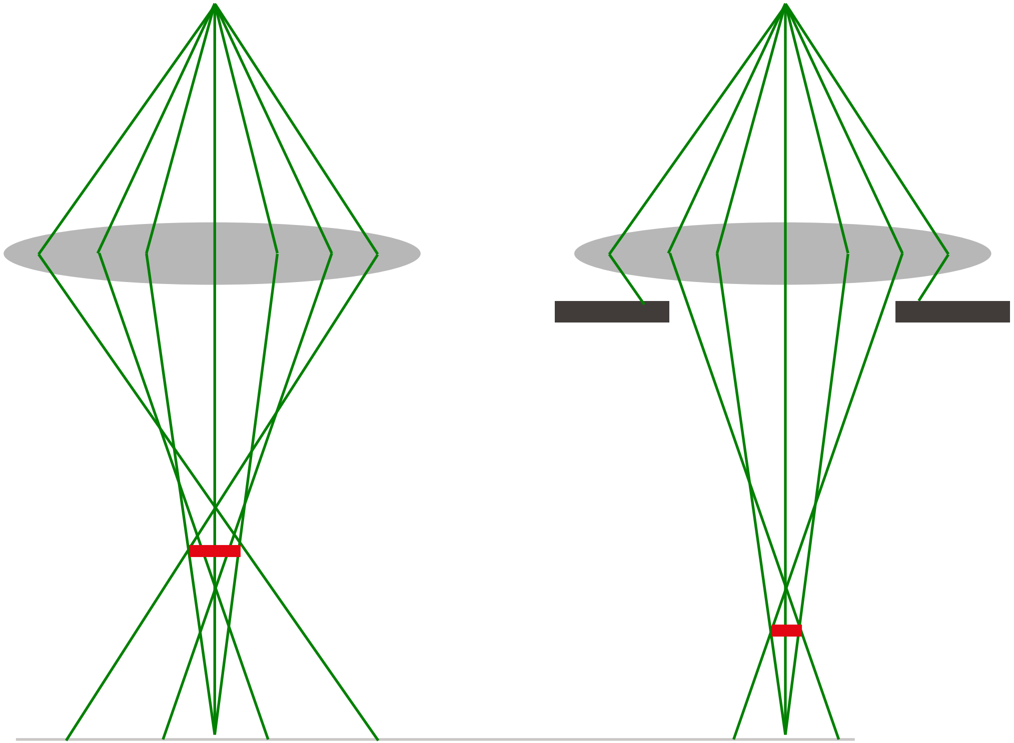

Inserting an aperture can lessen the effect of spherical aberration

But it comes with a cost → Lower current and more diffraction effect

Aberrations | Correctors

- Cs correction in light optics
  - Correction with combination of convex and concave lenses

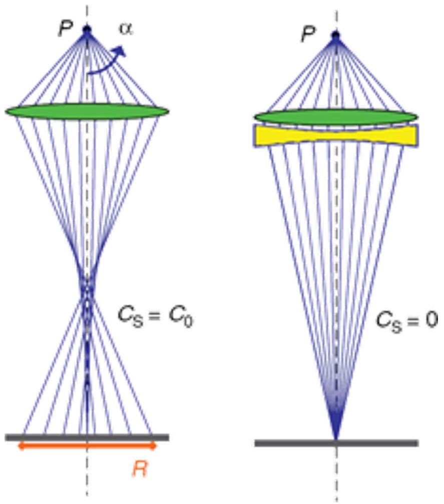

- Cs correction in electron optics
  - Combination of standard radially-symmetric convergent lenses with multipole divergent lenses (e.g. tetrapoles, hextapoles) to tune C_S.
  - Compensate Cs and other distortions with equivalnt but opposite componenets to add together with aim of giving ideal spherical wavefront.

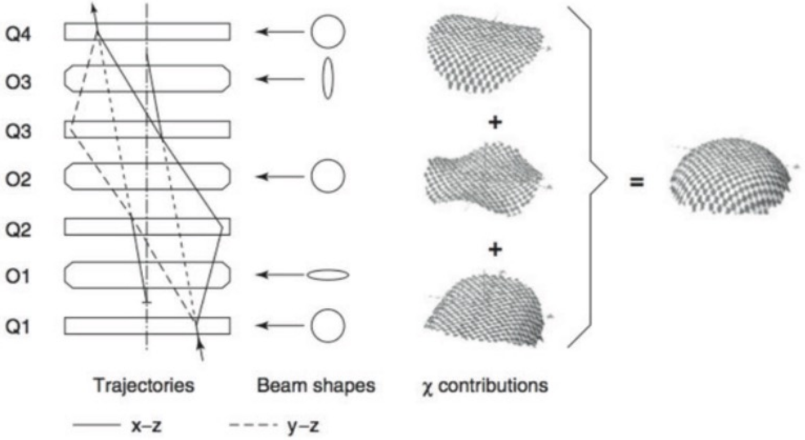

Krivanek et al. Aberration Correction in Electron Microscopy, Handbook of Charged Particle Physics 2009, pp. 601–641
http://www.sfc.fr/Material/hrst.mit.edu/hrs/materials/public/ElecMicr.htm

EPFL

Aberrations | Resolution

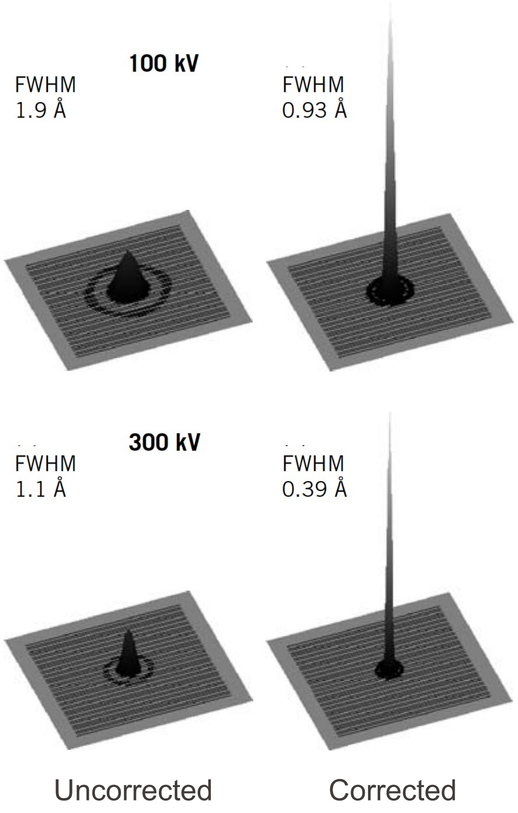

Z-contrast images

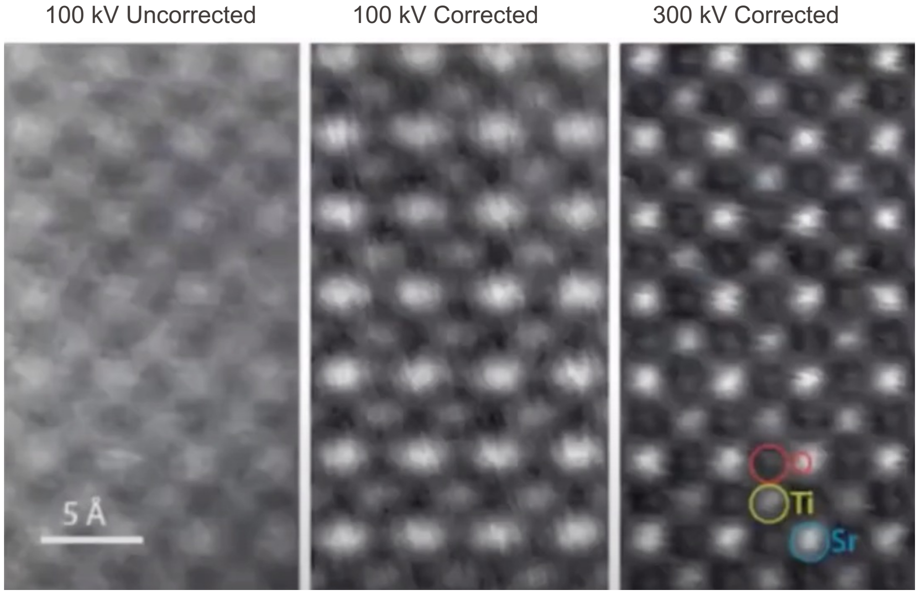

Advances in Imaging and Electron Physics 153, Peter W. Hawkes (Eds.)

Image formation

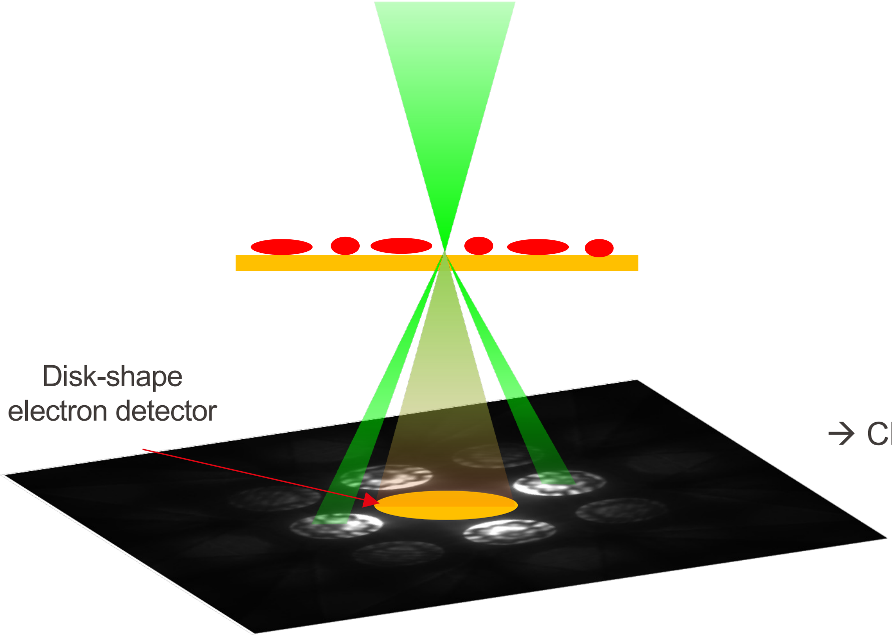

Scan position (x,y)

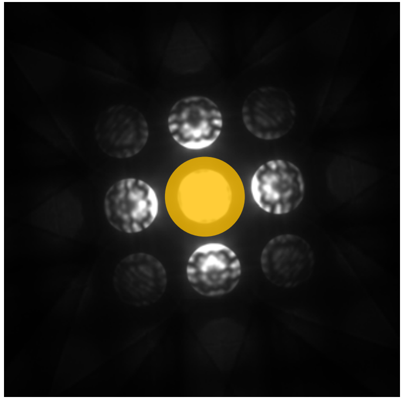

Defects, crystal tilts relative to incident or chenges in thickness,
→ Change in diffraction condition and intensities

→ Change in integrated signal on detector → Signal change on the image

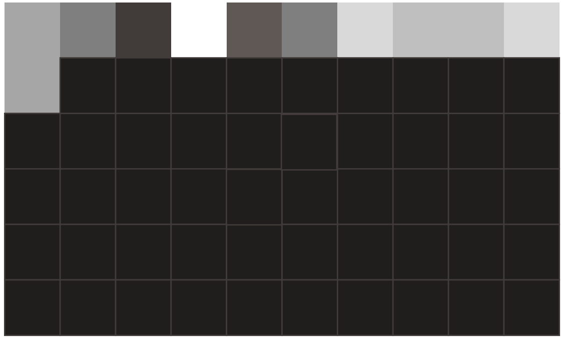

Image formation

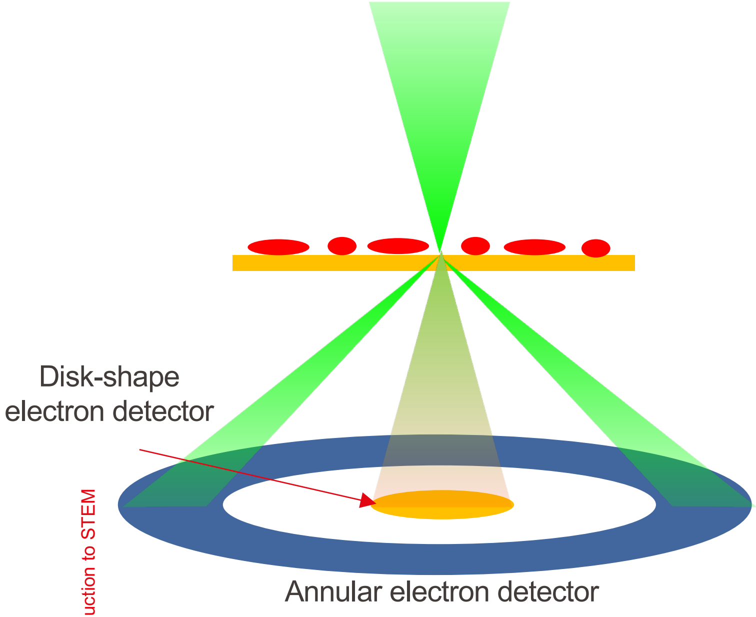

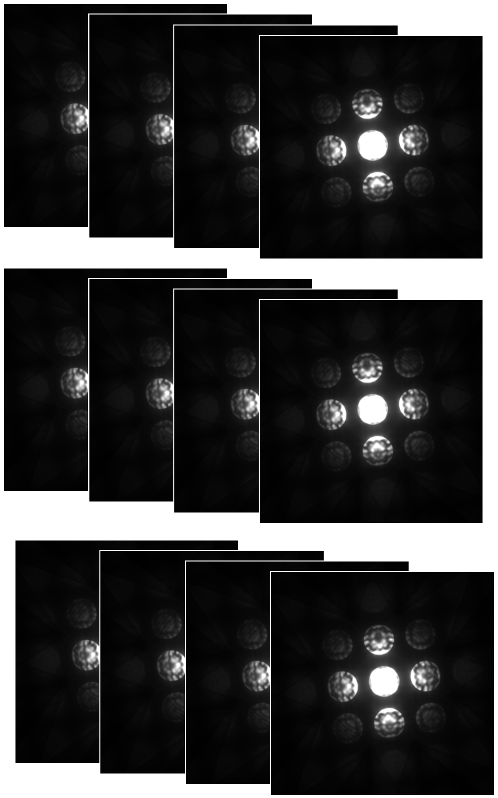

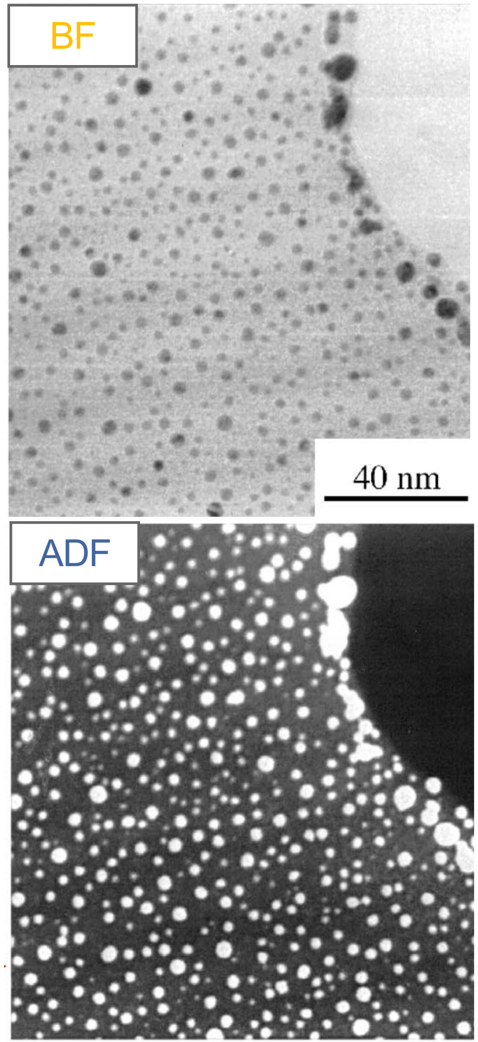

Principles of STEM | Knowledge of angles

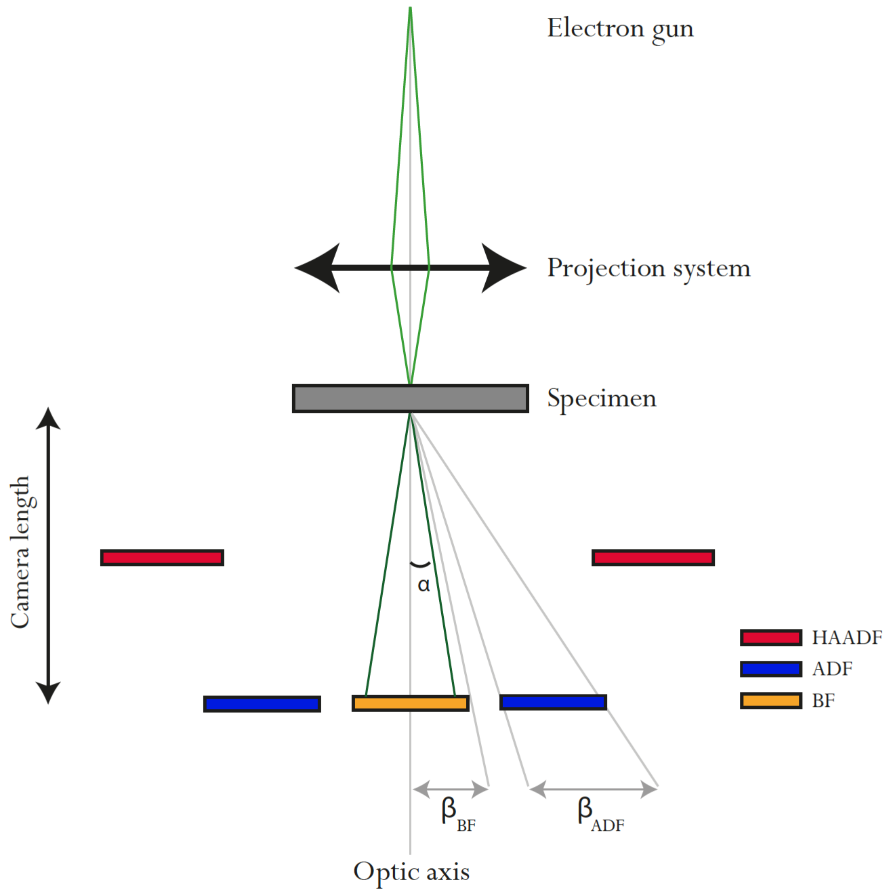

The focused probe is a convergent electron beam.

The BF and DF detectors are radially symmetric. Therefore all of them are characterised by angles – angle of convergence for the beam; collection of scattering angles for the detectors

The convergence semi-angle of the probe is called **α**

A collection semi-angle for a detector is called β

Knowledge of these angles is important for STEM imaging

Principles of STEM | Knowledge of angles

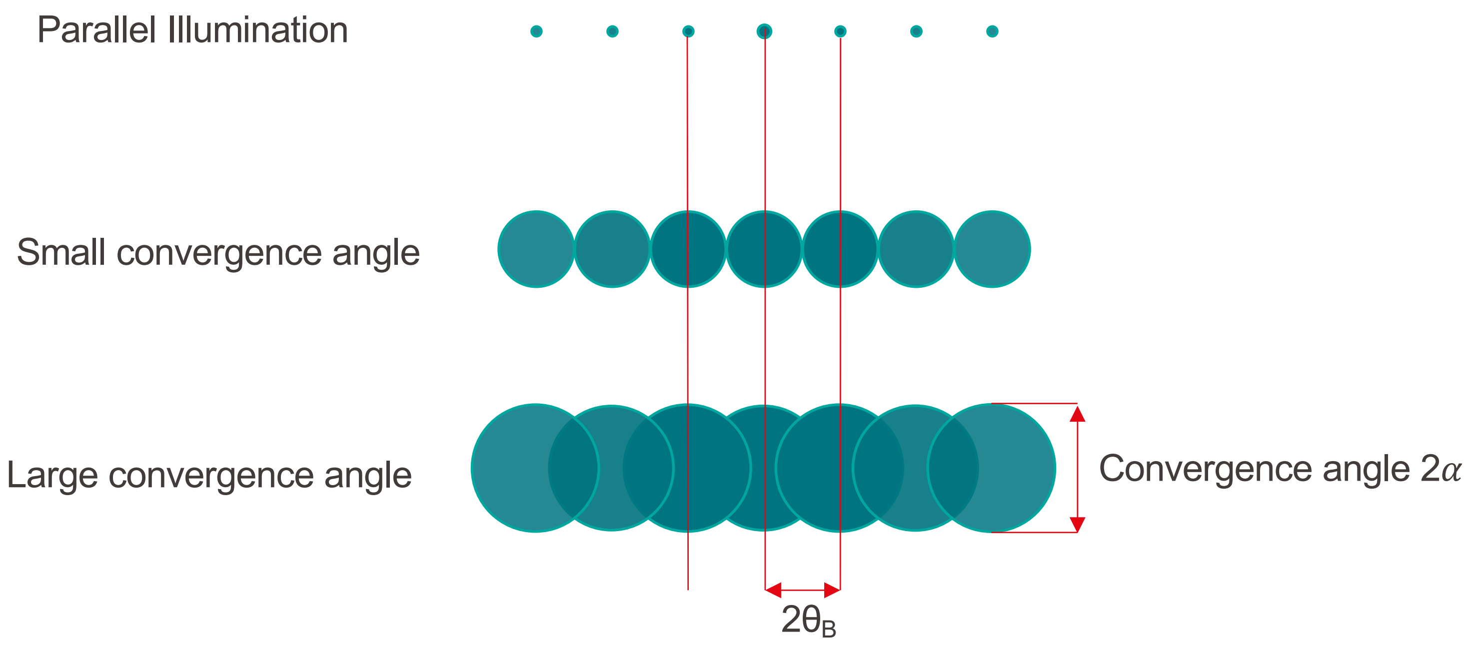

Disks overlap if $\theta_B < \alpha$

Principles of STEM | Knowledge of angles

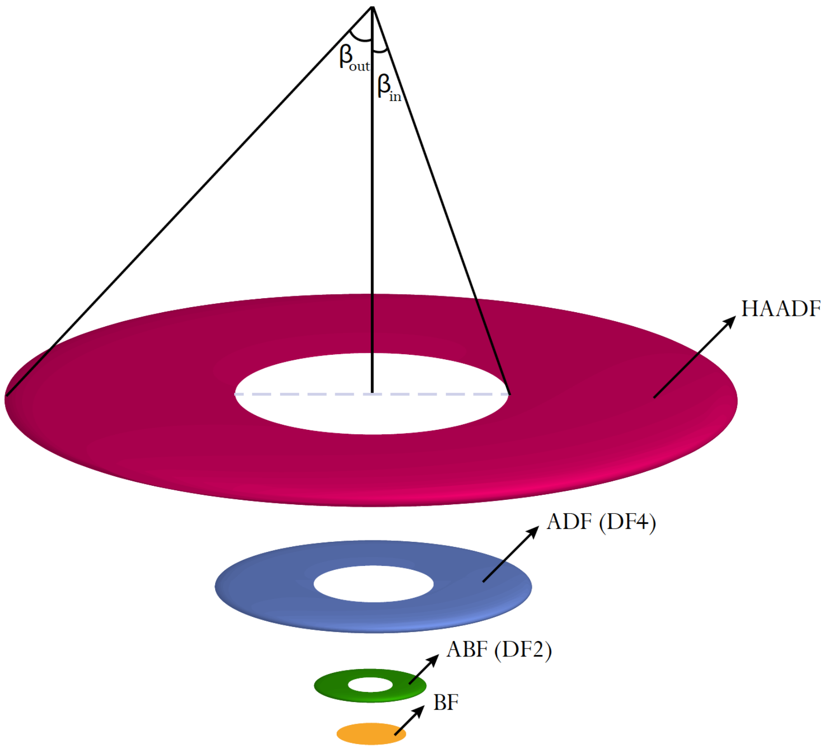

Schematic showing the configuration of the STEM detectors in the Tecnai-Osiris and Titan-Themis installed at CIME.

Principles of STEM | Knowledge of angles

Emad Oveisi

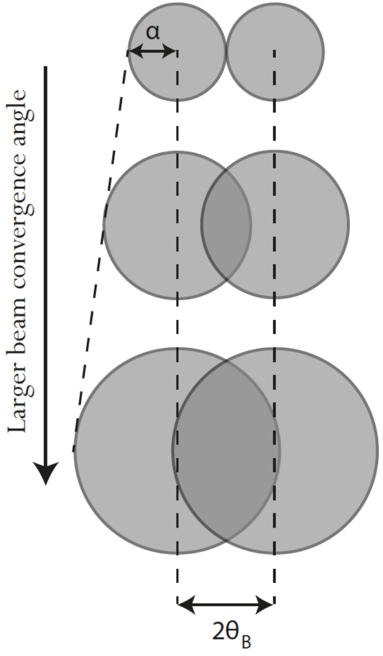

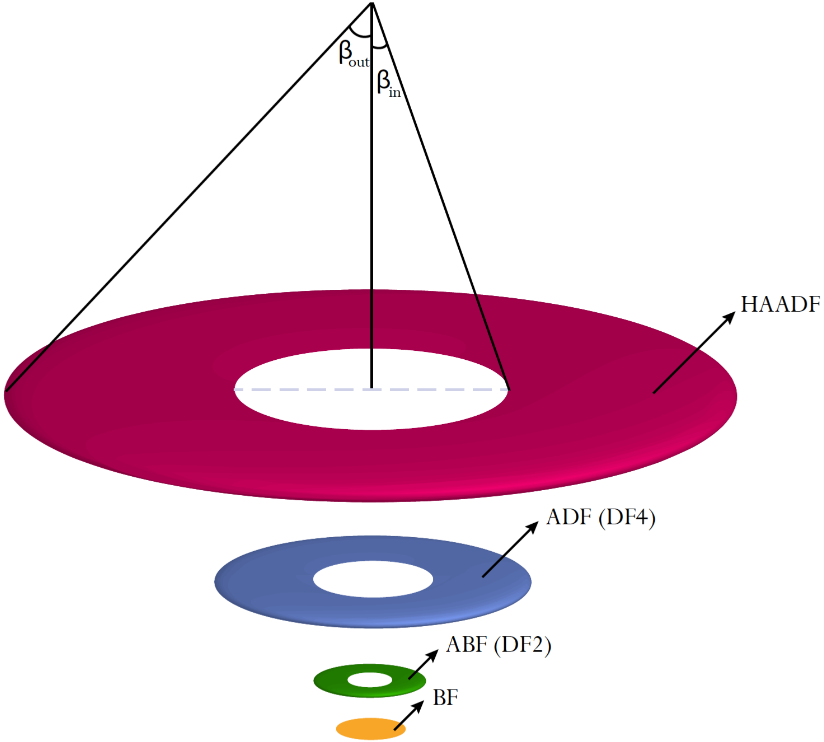

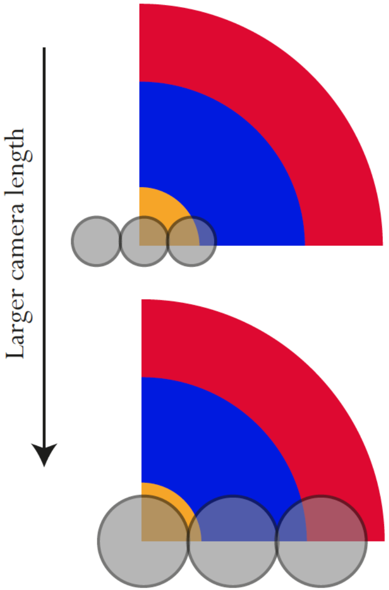

Principles of STEM | Knowledge of angles

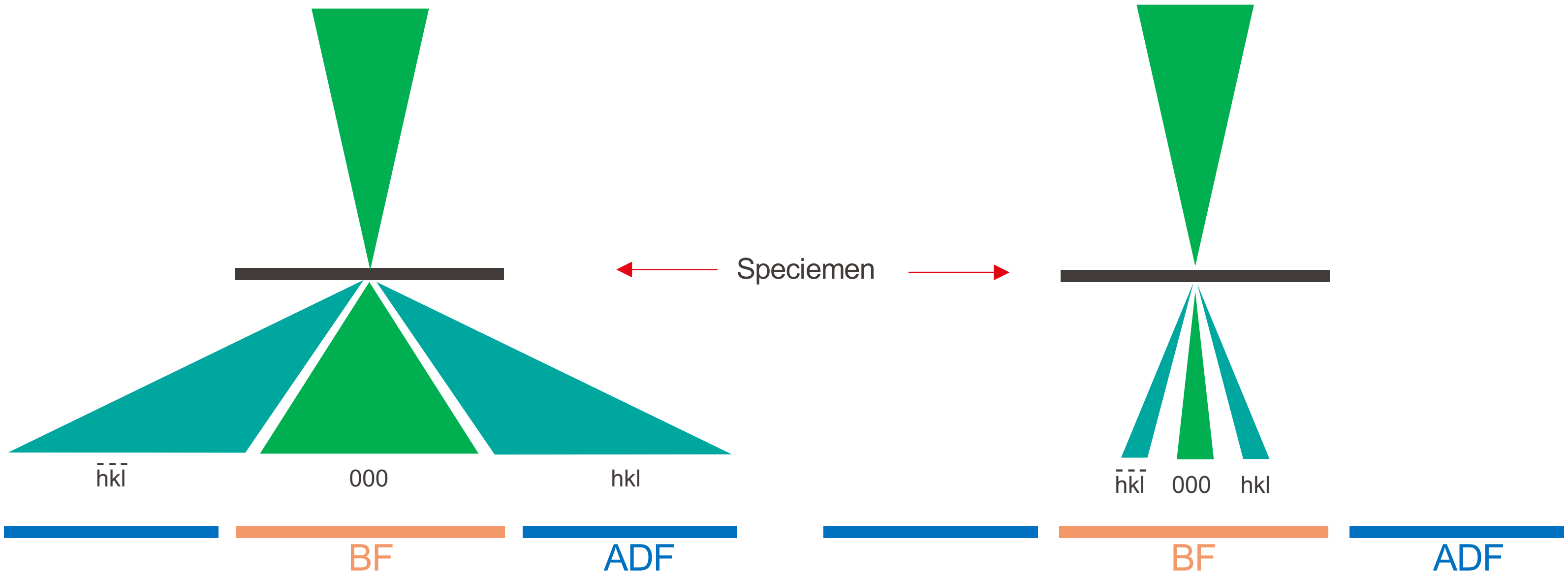

Large camera length

Small camera length

Imaging modes

Emad Oveisi

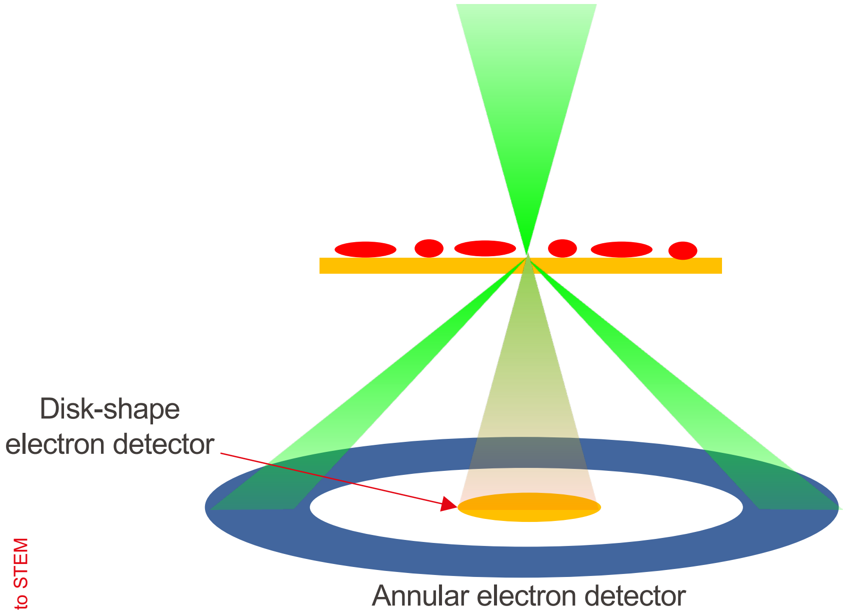

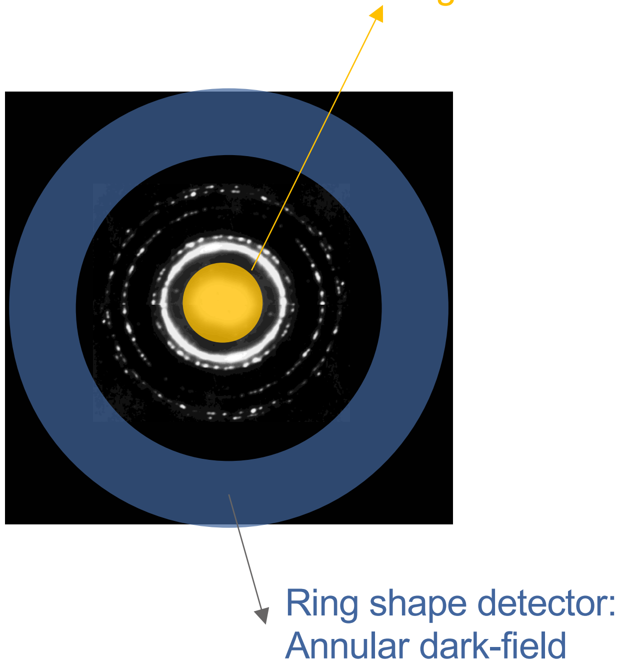

Imaging modes

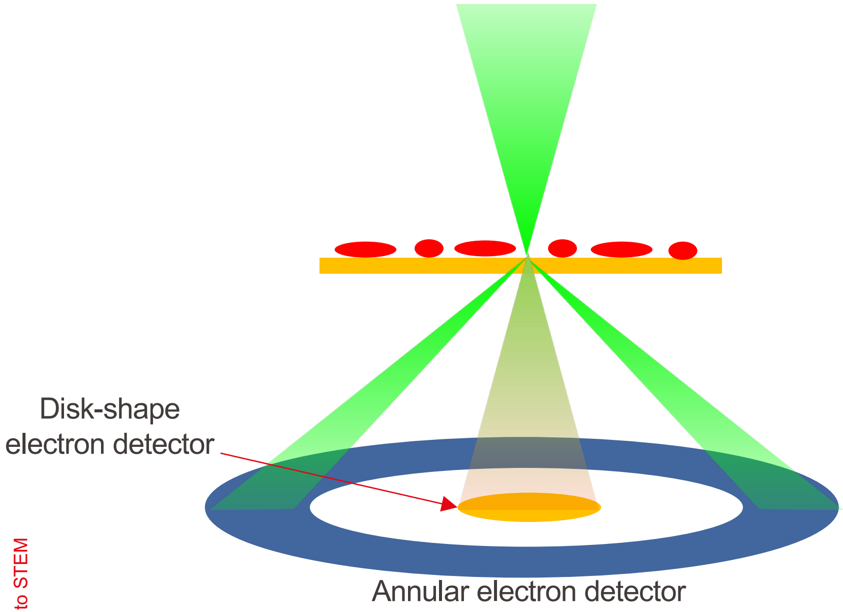

BF detector is a solid disc that picks up the direct beam which varies in intensity depending on the specific point on the specimen illuminated by the probe at that specific time.

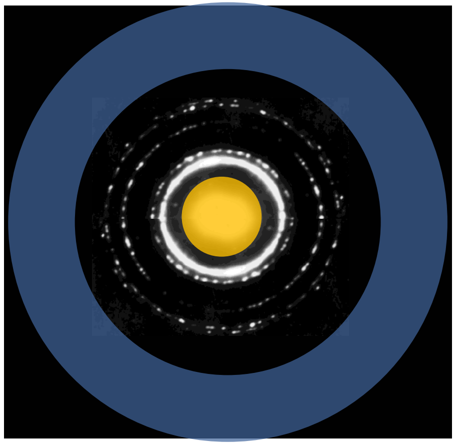

- Bright-field: On axis | Electrons pass throught the sample without being scattered → Coherent imaging

Imaging modes

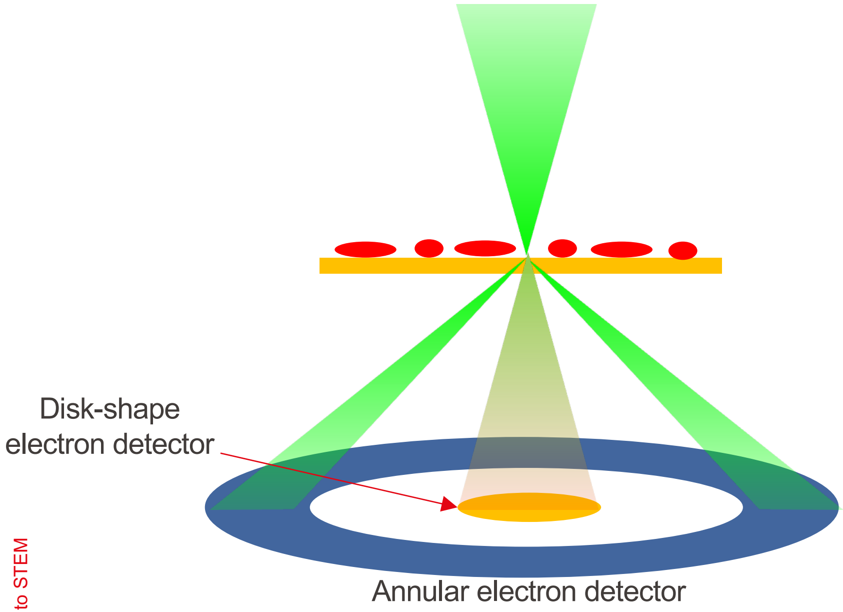

For dark-field imaging, we use an annular detector, with certain inner and outer collection semi-angles, which surrounds the BF detector, and then all the scattered electrons fall onto that detector.

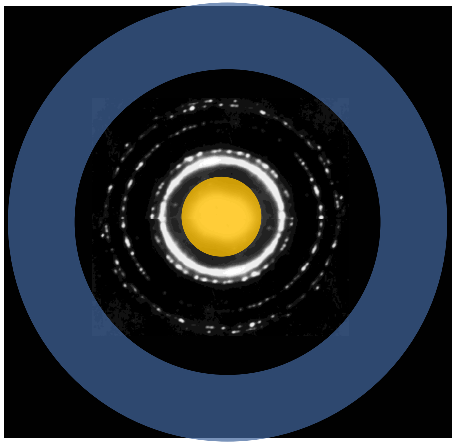

- Annular dark-field: Off-axis | Electrons diffracted off axis by ineraction with the sample → Incoherent imaging

Imaging modes | Annular dark-field

- Proposed by Crewe and co-workers during the initial development of the modern STEM.

- Detector consists of an annular sensitive region that detects electrons scattered over an angular range. The radii can both vary over a large range, but typically the inner radius would be in the range of 30–100 mrad and the outer radius 100–200 mrad.

- High scattering angles (>~100 mrad) would enhance the compositional contrast and that the coherent effects of elastic scattering could be neglected because the scattering was almost entirely thermally diffuse → Incoherent imaging

Imaging modes

Emad Oveisi

Bright-field TEM

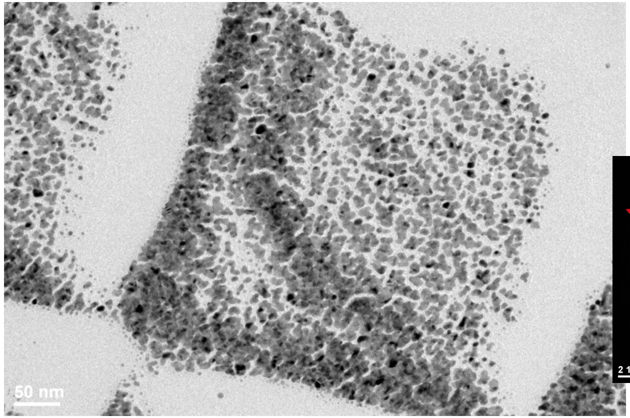

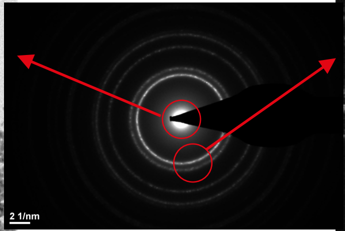

Aperture

Dark-field TEM

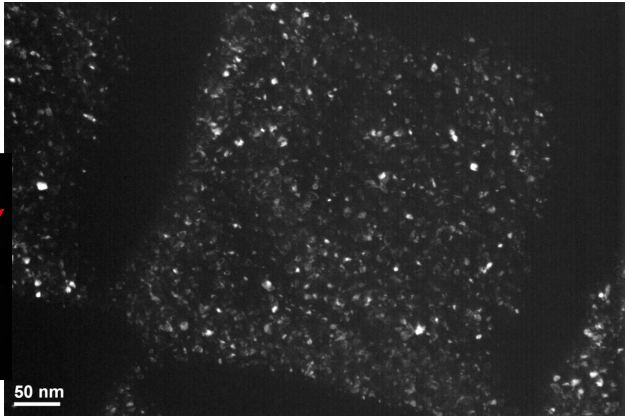

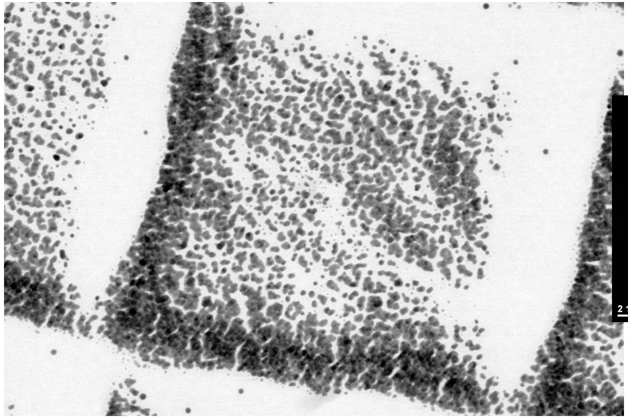

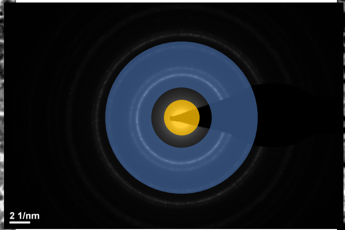

Detector

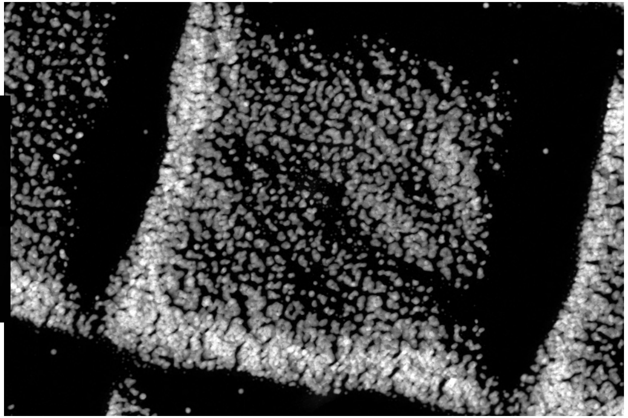

Bright-field STEM

Annular dark-field STEM

Imaging modes

ADF-STEM and DF-TEM images of a photovoltaic stack

Visible: Protocrystalline/crystalline Si interface, B-doped layer in proto-Si, voids

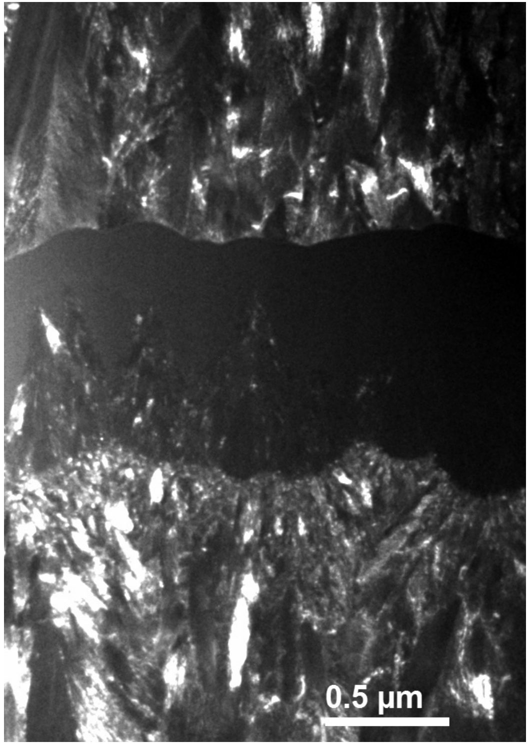

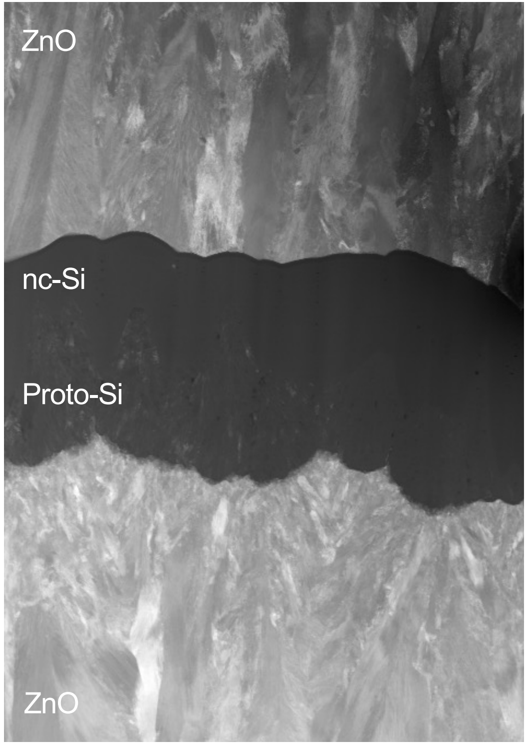

Which one is the annular dark-field STEM image?

Slide courtesy of D.T.L. Alexander, EPFL

Imaging modes

ADF-STEM and DF-TEM images of a photovoltaic stack

Visible: Protocrystalline/crystalline Si interface, B-doped layer in proto-Si, voids

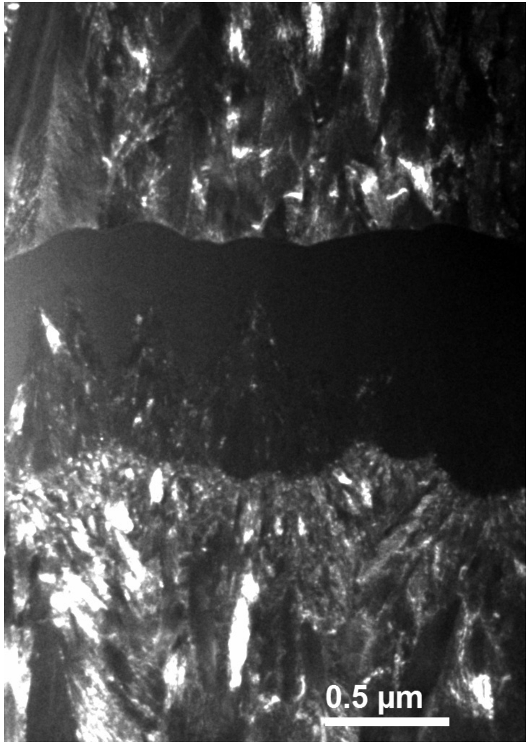

Few grains have intensity
strong contrast

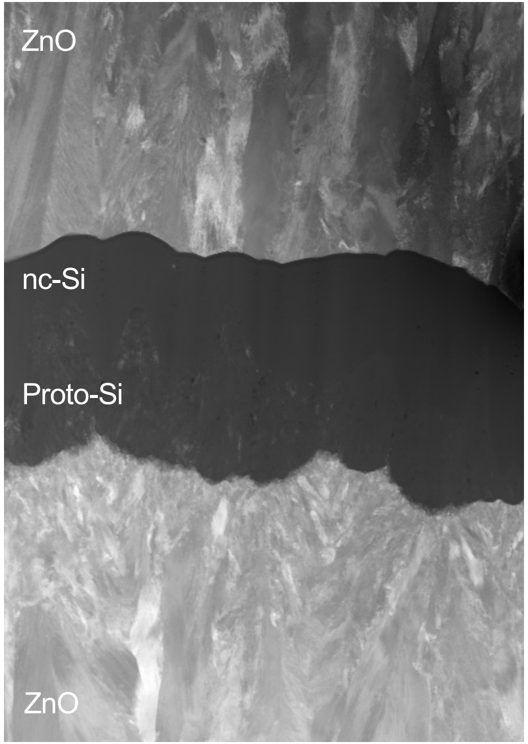

More grains have intensity
More grain visibility & less contrast

Slide courtesy of D.T.L. Alexander, EPFL

Imaging modes | High-angle annular dark-field

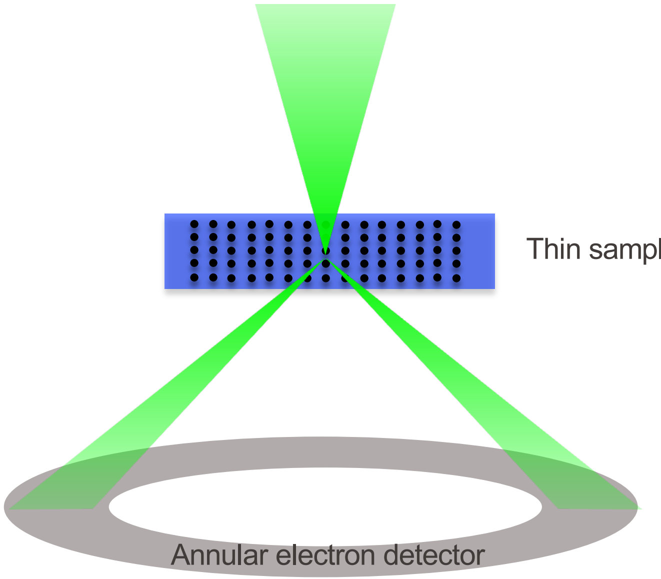

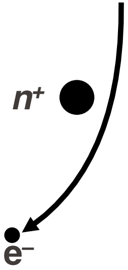

Rutherford-type scattering from nucleus (thermal diffuse scattering = TDS)

High-angle annular dark-field (HAADF) image

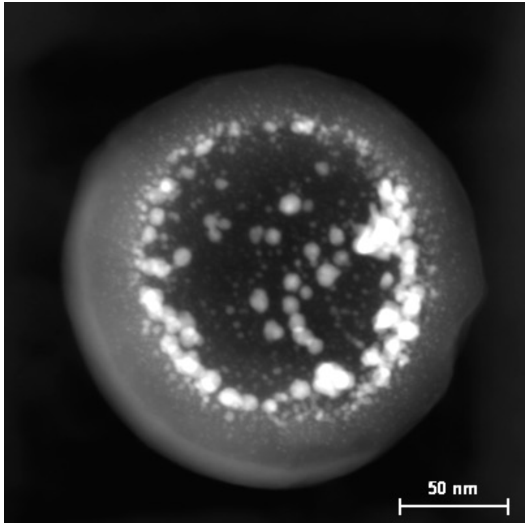

Ni-Rh catalytic nanoparticles in carbon shell

Mass/thickness contrast image

- Incoherent Rutherford-type scattering deflects transmitted e^- to high angle of scattering;
- larger nucleus / thicker the specimen → more scattering
- Map image intensity as function of probe position *(x, y)*
- Image intensity: $I(x, y) \propto t * Z^{1.6-2}$

Imaging modes | High-angle annular dark-field

Cs-corrected atomic resolution HAADF-STEM of perovskite interface (300 kV)

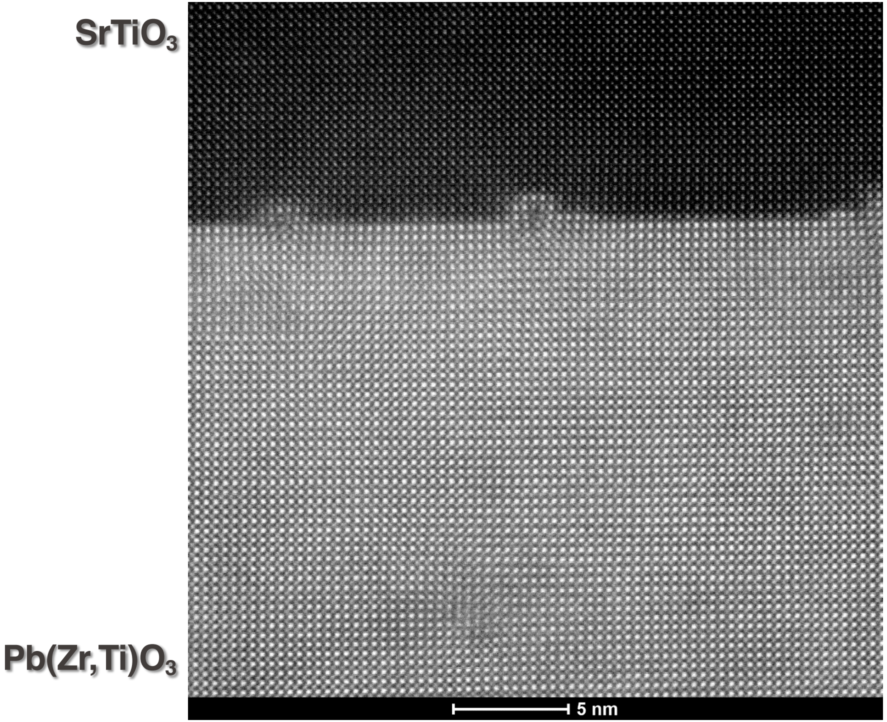

Imaging modes | High-angle annular dark-field

Cs-corrected atomic resolution HAADF-STEM of perovskite interface (300 kV)

$SrTiO_3$

$Pb(Zr,Ti)O_3$

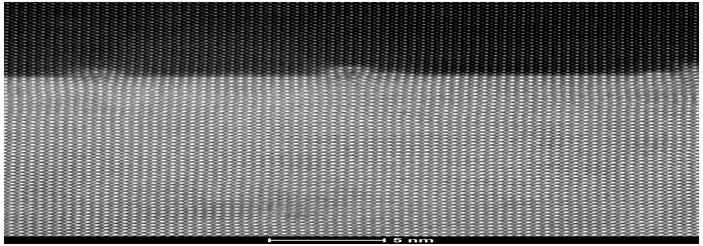

Imaging modes | High-angle annular dark-field

$YBa_2Cu_3O_{7-\delta}$ $ErBa_2Cu_3O_{7-\delta}$,

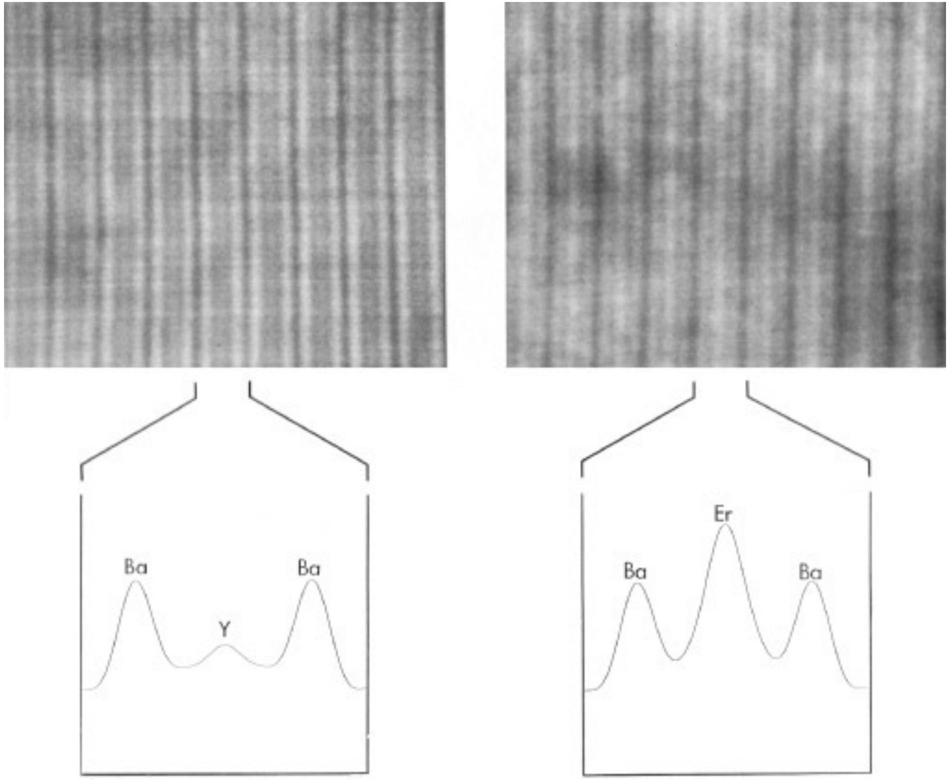

Pennycook S.J., Ultramicorscopy (2017) 180, 22-33.

Imaging modes | High-angle annular dark-field

HAADF image showing individual Pt atoms in a zeolite framework

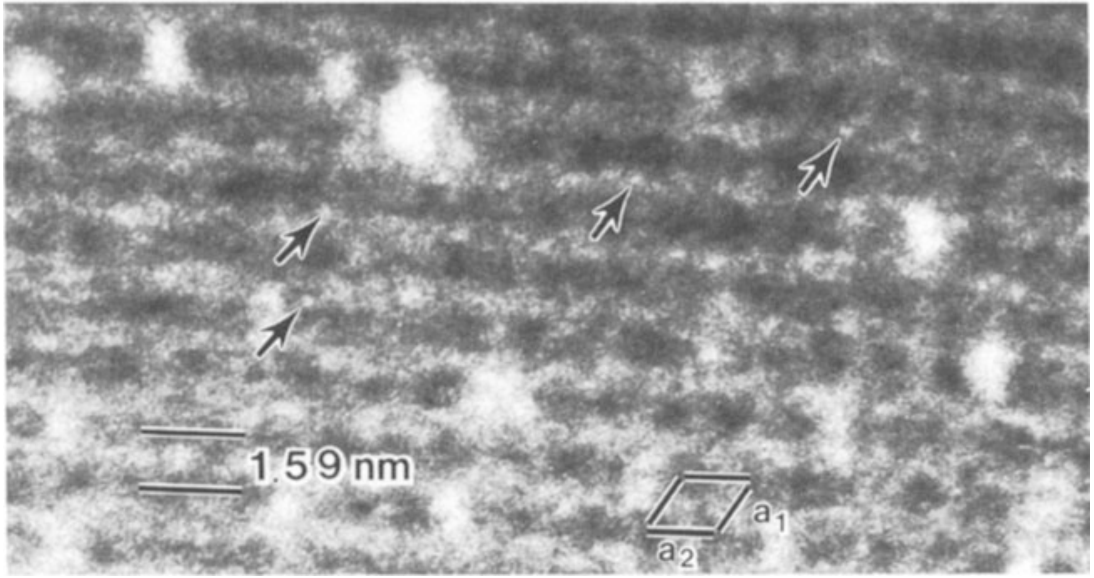

Rice *et al.* (1990).

Imaging modes | High-angle annular dark-field

Pt clusters inside a metallosupramolecular polymer

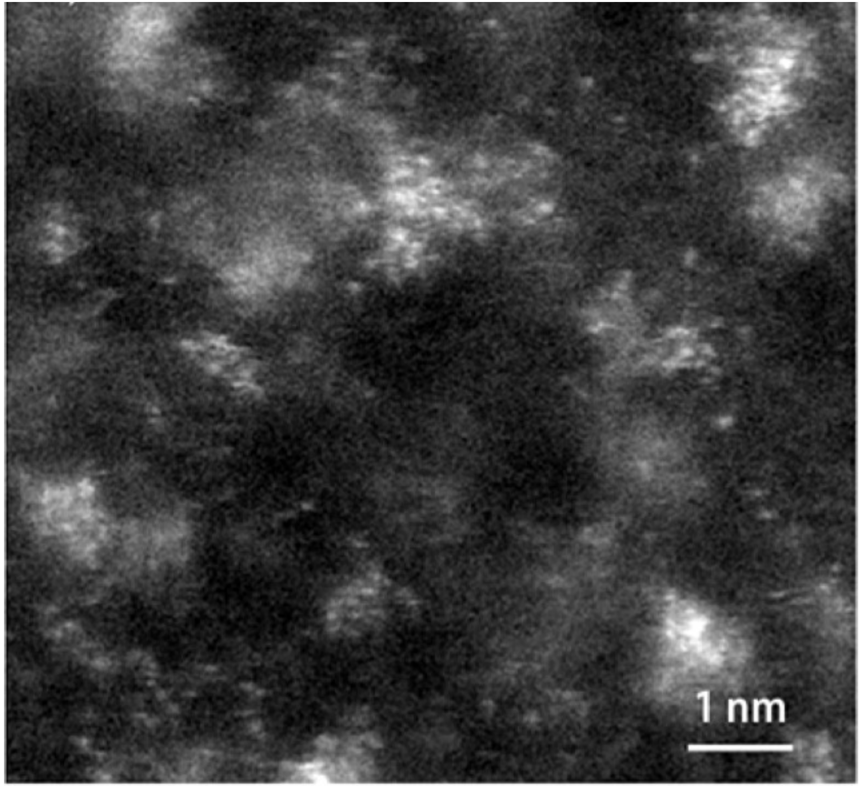

In collaboration with Adolphe Merkle Institute.
Olaeche *et al.*, JACS 2020.

Imaging modes | High-angle annular dark-field

In / Ga multilayer

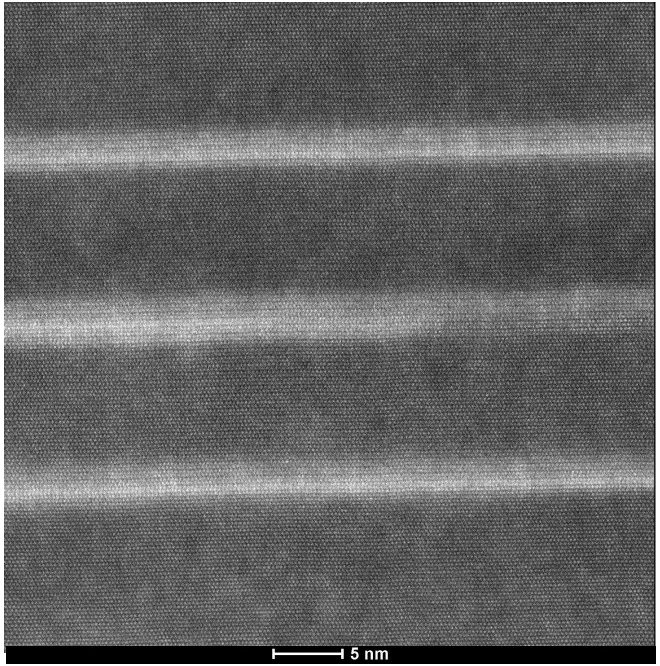

Evaluated map of the In concentration

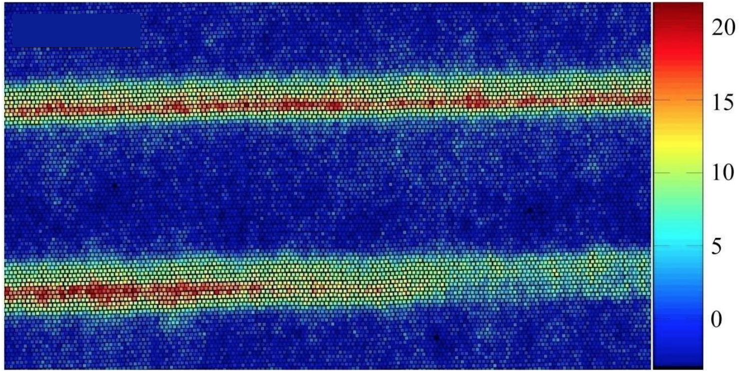

Quantitative STEM allows measurement of composition

Requires detector calibration

Imaging modes | High-angle annular dark-field

Ag cluster embedded in an Al matrix together with the number of Ag atoms per column

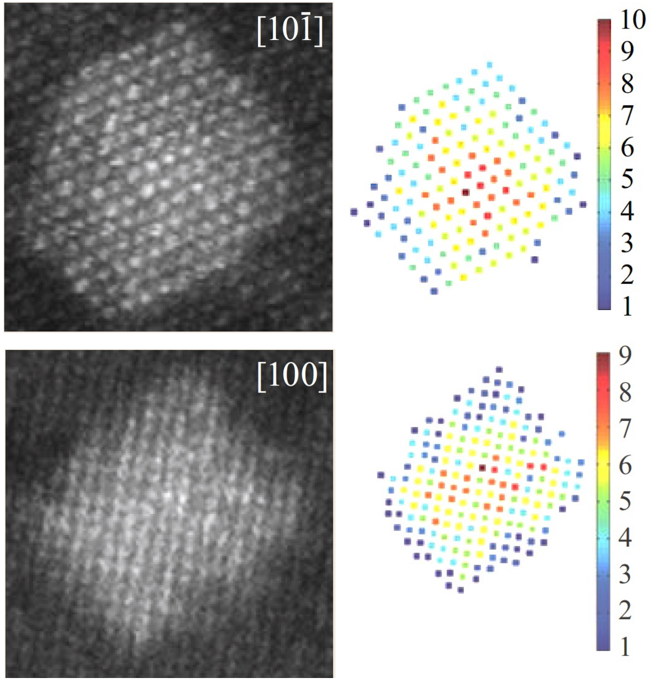

Computed 3-D reconstruction of the cluster viewed along three different directions

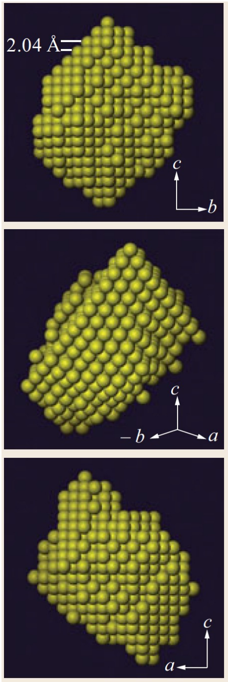

Atom counting implies precise detector calibration and assumptions about the sample

S. Van Aert *et al.*, Nature 470, 374– 377 (2011).

Emad Oveisi

Imaging modes | High-angle annular dark-field

Example : Variation of the intensity according to the number of graphene layers

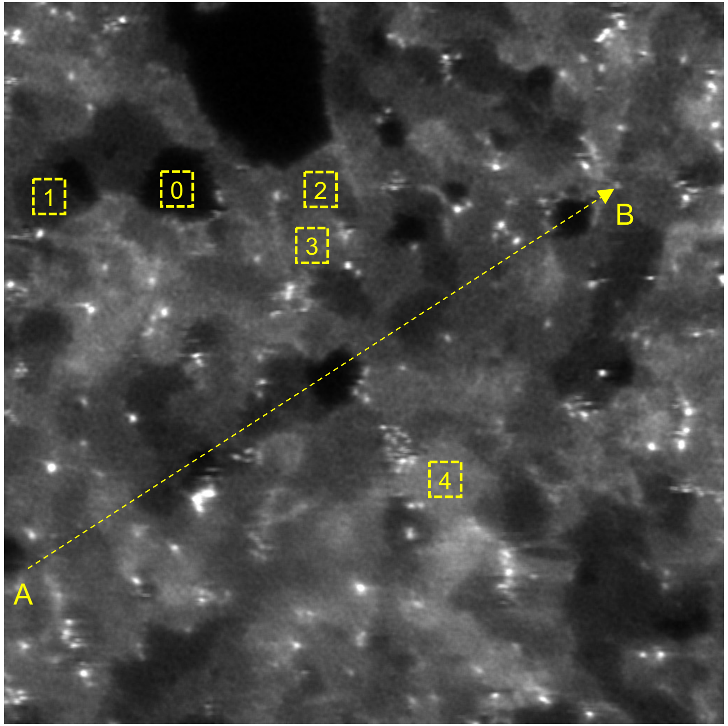

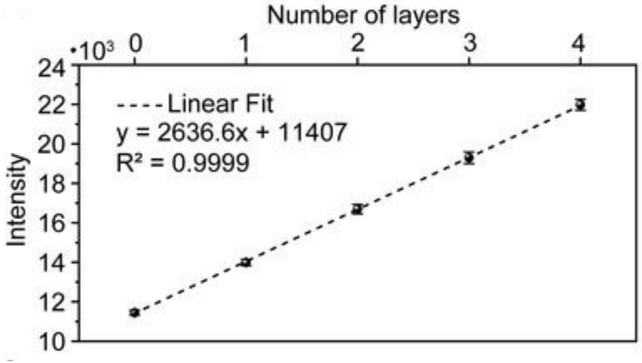

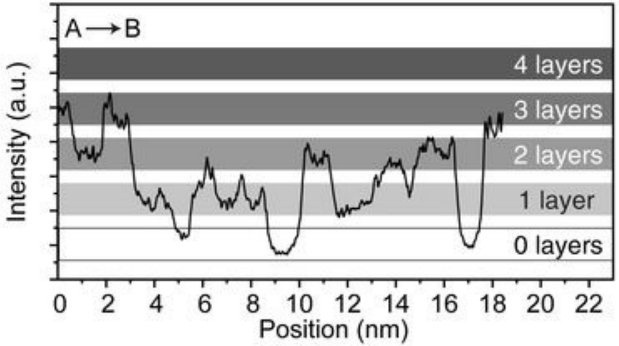

In collaboration with LAS, EPFL.
Luis Francisco Villalobos *et al.* PNAS 2021

Imaging modes | Effect of camera length

High camera lengh

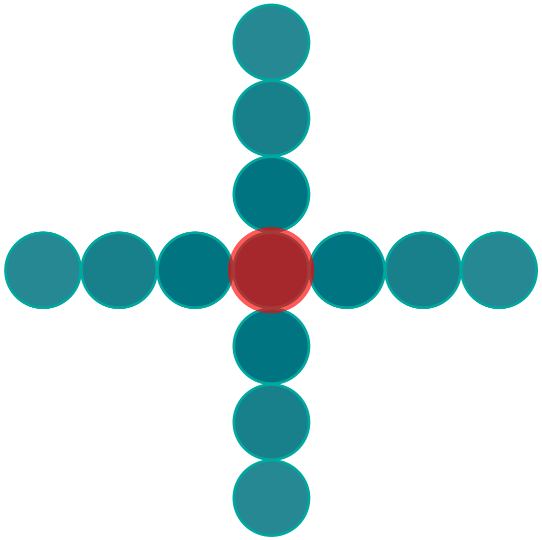

Low camera lengh

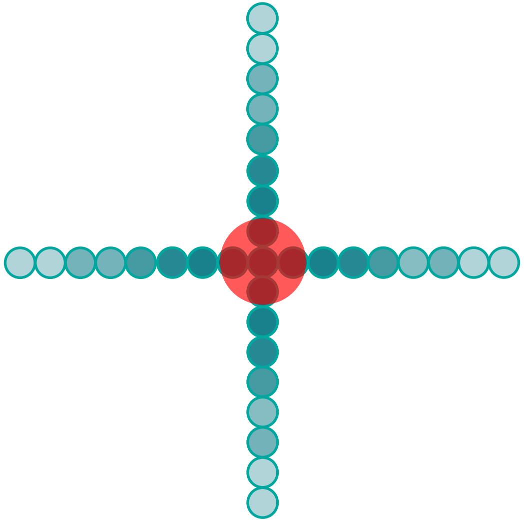

Direcly tranmistted disk on the solid disk detector
→ BF-STEM image

Both direct and diffracted disks
on the the solid disk detector

Imaging modes | Effect of camera length

Emad Oveisi

High camera lengh

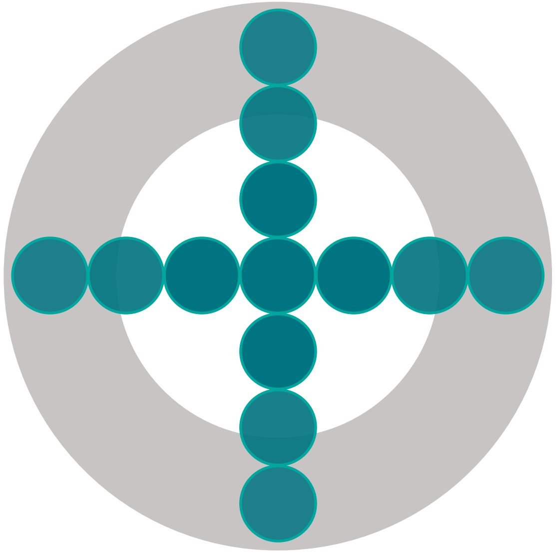

Dominant diffraction contrast

Low camera lengh

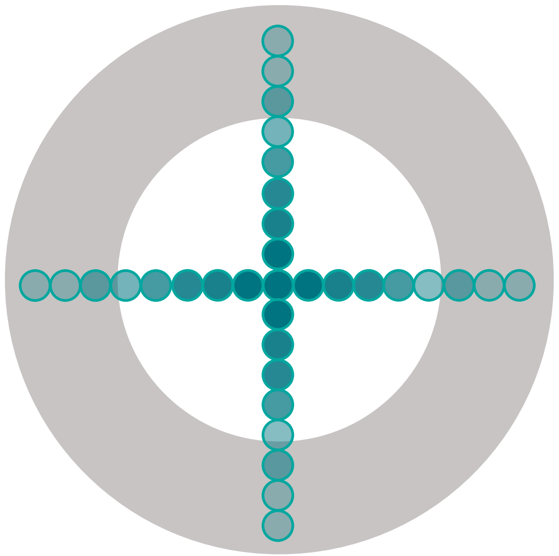

Dominant Z-contrast (TDS)

Imaging modes | Effect of camera length

High camera lengh

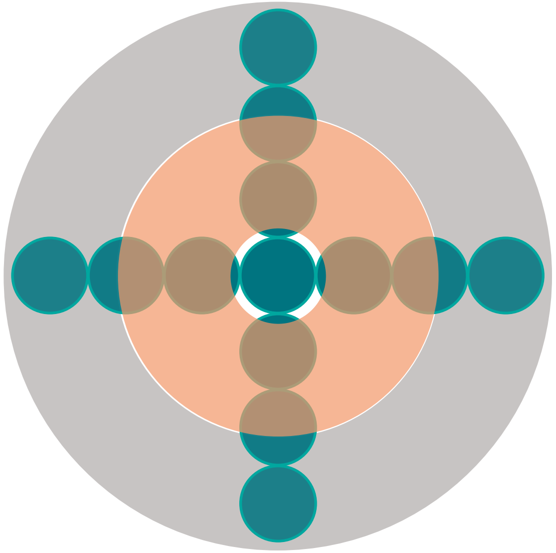

Mixed diffraction and Z-contrast → MAADF

Pure diffraction contrast → LAADF

Low camera lengh

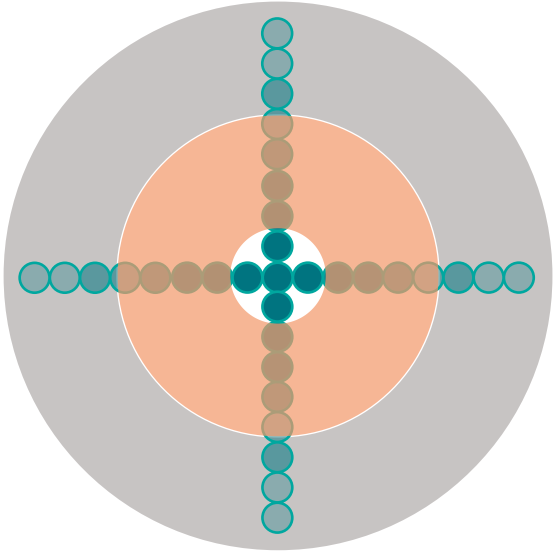

Z-contrast image → HAADF

Mixed diffraction and Z-contrast → MAADF

Imaging modes | Effect of camera length

High camera lengh

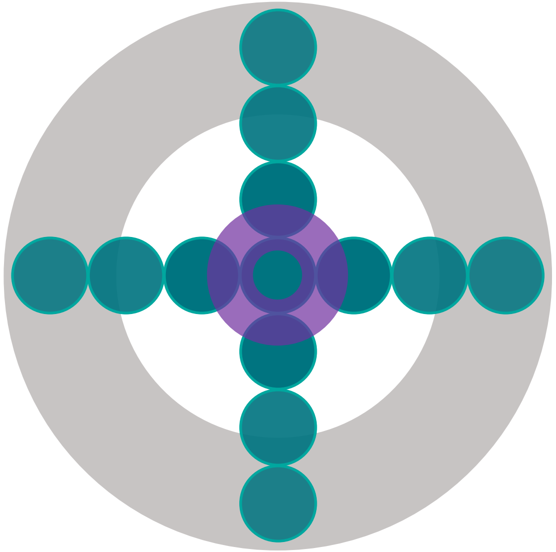

Mixed diffraction and Z-contrast → MAADF

Annular bright-field (ABF) image

Low camera lengh

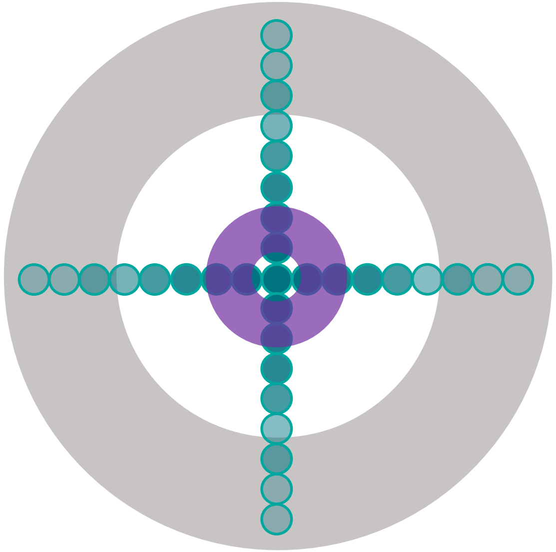

Z-contrast image → HAADF

Pure diffraction contrast → LAADF

Imaging modes | Effect of camera length

Emad Oveisi

High camera lengh

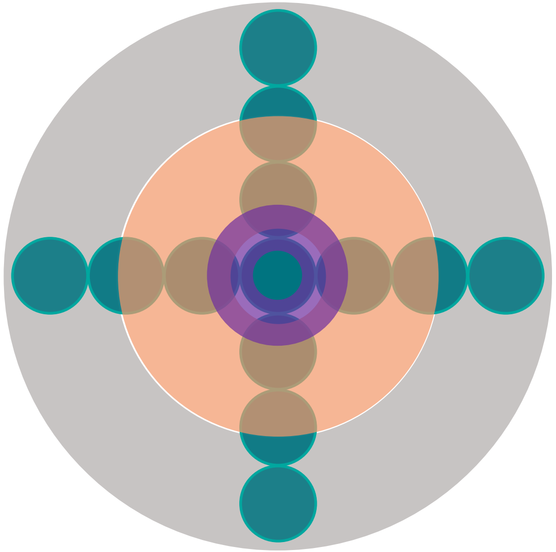

Mixed diffraction and Z-contrast → MAADF
Pure diffraction contrast → LAADF
Annular bright-field (ABF) image

Low camera lengh

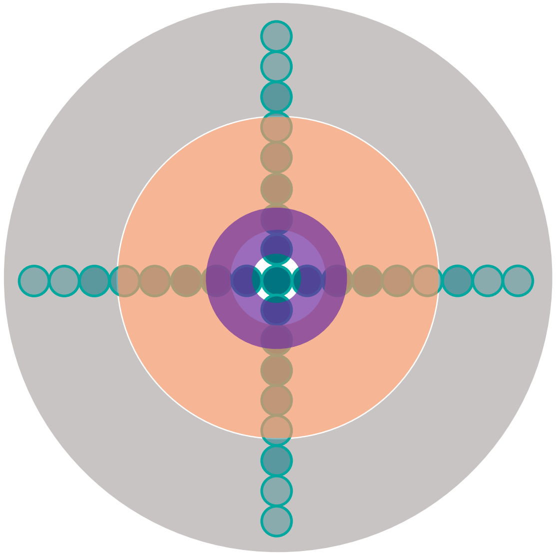

Z-contrast image → HAADF
Mixed diffraction and Z-contrast → MAADF
Pure diffraction contrast → LAADF

Imaging modes | Low-angle annular dark-field

Example: Variation of defect contrast with camera length in ɣ / ɣ' region of Ni-superalloy

HAADF

MAADF

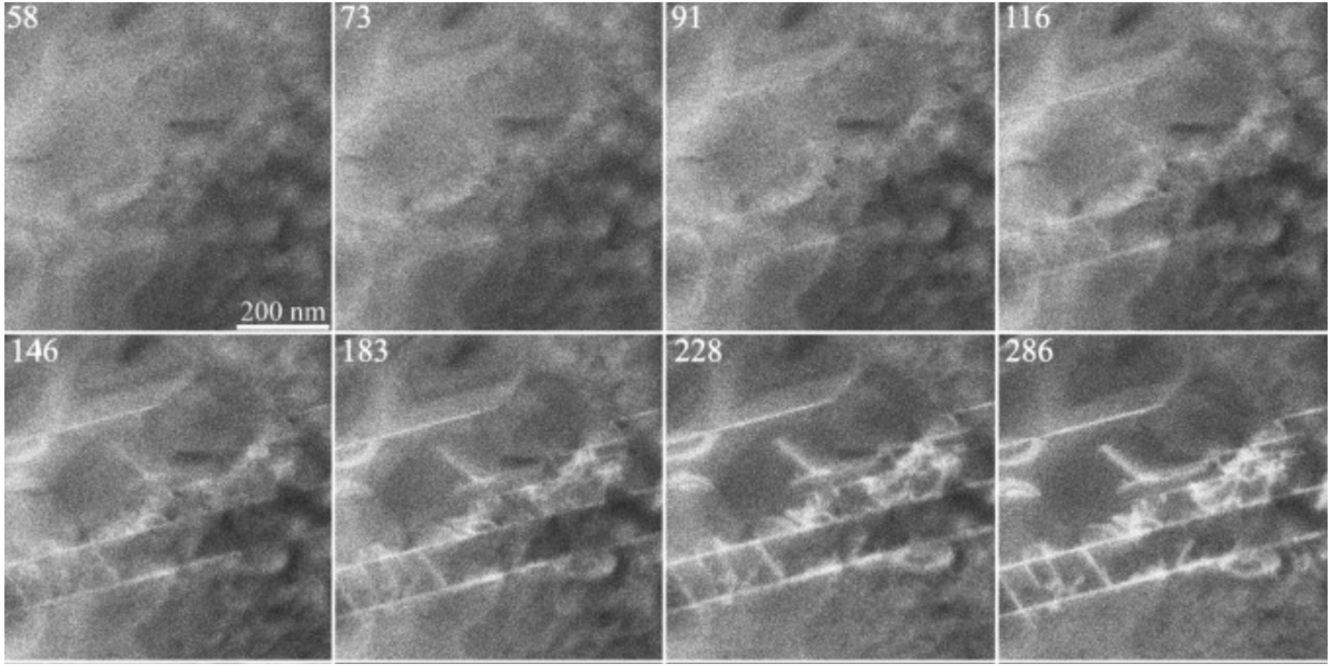

MAADF

LAADF

Philips *et al.*, Ultramicorscopy 2012.

Imaging modes | Medium-angle annular dark-field

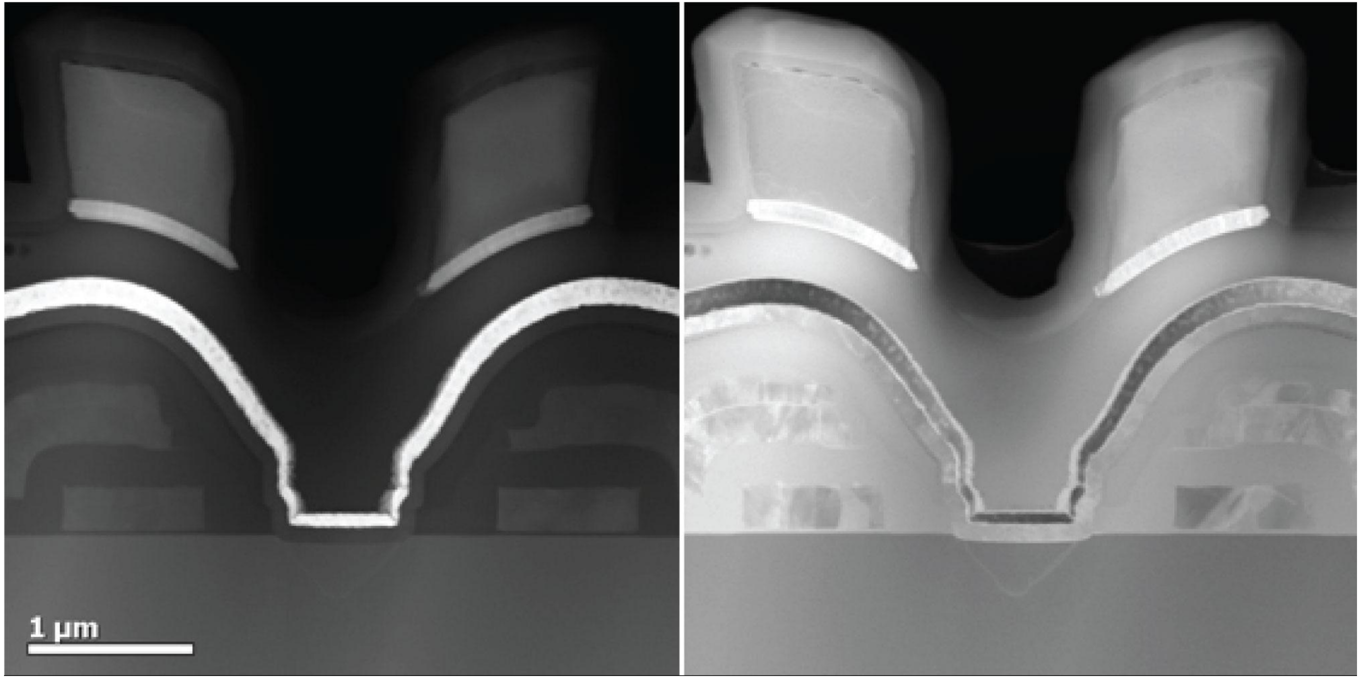

Jointly acquired HAADF and MAADF signals

The HAADF signal (left) contrast is easily interpreted in terms of mass thickness of the material while the diffraction contrast MAADF signal (right) reveals highly detailed structural changes in the material. The optimized geometry makes this possible.

https://www.gatan.com/products/tem-imaging-spectroscopy/advanced-stem-detectors

Imaging modes | Medium-angle annular dark-field

Example: Doped graphene, BN monolayer – C_S STEM

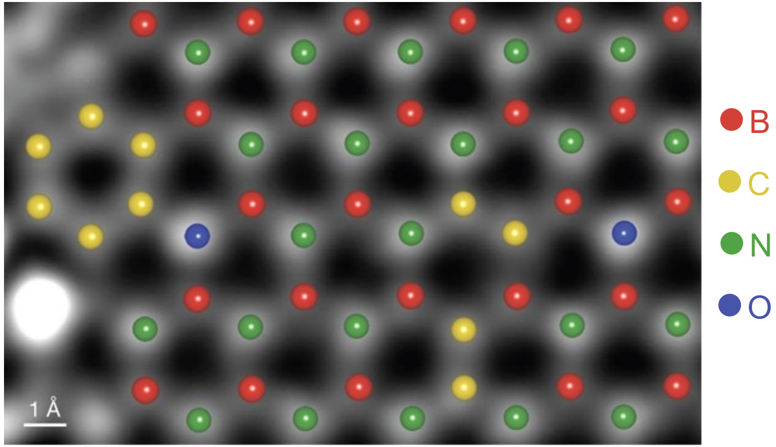

Low kV essential to prevent knock-on damage; here 60 kV used

As λ increases aberration correction even more important for obtaining atomic resolution

Medium-angle ADF gives intensity $I \propto Z^{1.7}$ but with increased signal intensity compared to true HAADF image. This intensity is needed for imaging single atom by single atom (here β = 58–200 mrad)

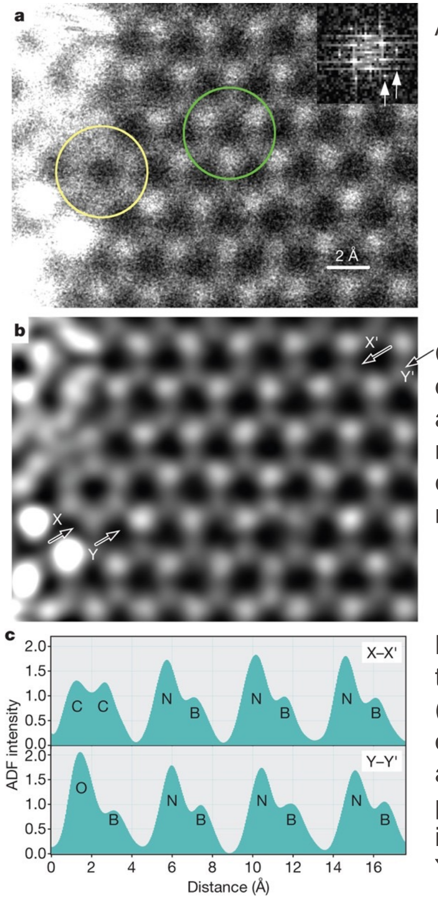

As recorded.

Corrected for distortion, smoothed, and deconvolved to remove probe tail contributions to nearest neighbours.

Line profiles showing the image intensity (normalized to equal one for a single boron atom) as a function of position in image **b** along X–X′ and Y–Y′.

Krivanek, *et al.* Nature **464** (2010).

Imaging modes | Coherent vs incoherent image

Definition of incoherent imaging: the image gives a representation of the object, which is blurred by the size of the probe.

i.e. “The sharper the probe, the clearer the atoms appear. Different atoms will have spikes with different heights, dependent on their cross-sections, which are roughly proportional to Z^2. As the probe is focused and defocused the atoms come into clear view and blur out again
→ Camera-like characteristic.

Example: Si <110>

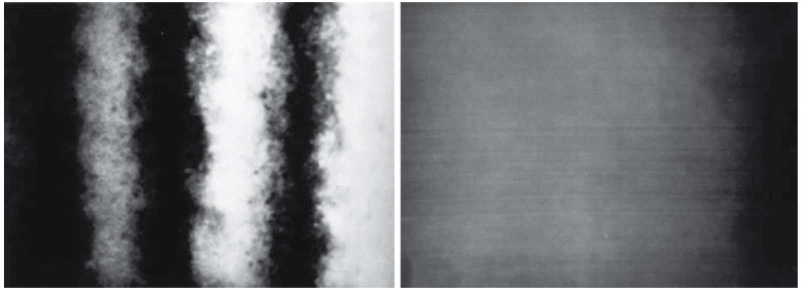

BF-STEM: Thickness fringes visible
→ Coherent

Z-contrast image
→ Incoherent

Ultramicroscopy, 37 (1991), pp. 14-38

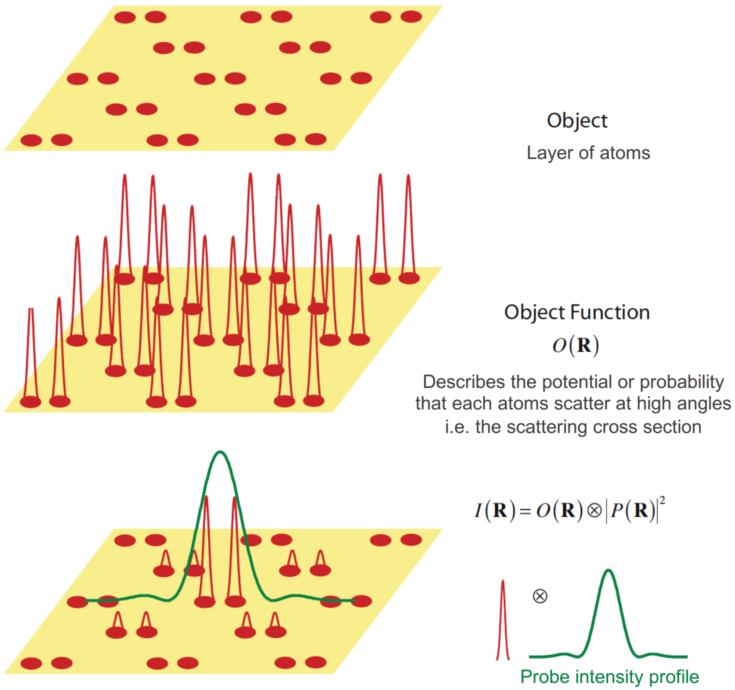

Incoherent:
All phase relationships between electrons ‘emitted’ (in reality scattered) between one atom and the next are random, and each atom can be considered an incoherent source of diffuse scattering.

EPFL

Imaging modes | Coherent vs incoherent image

BF-TEM

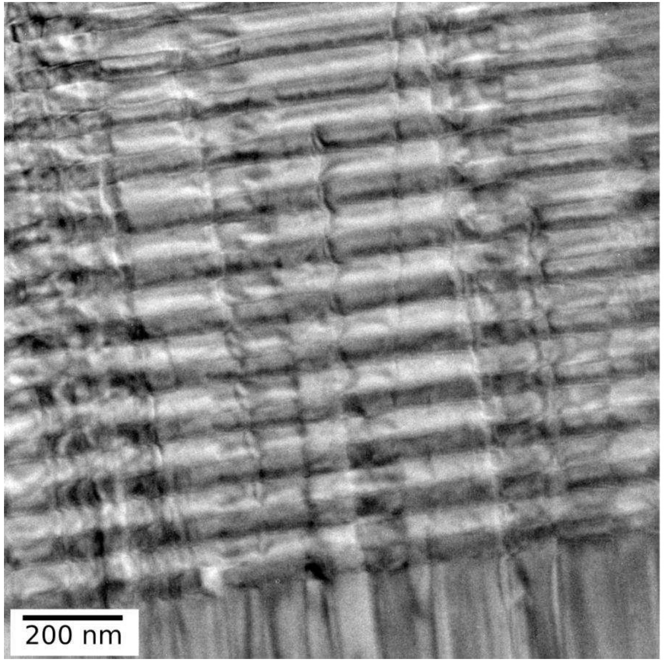

Contrast due to strain and diffraction effects

HAADF-STEM

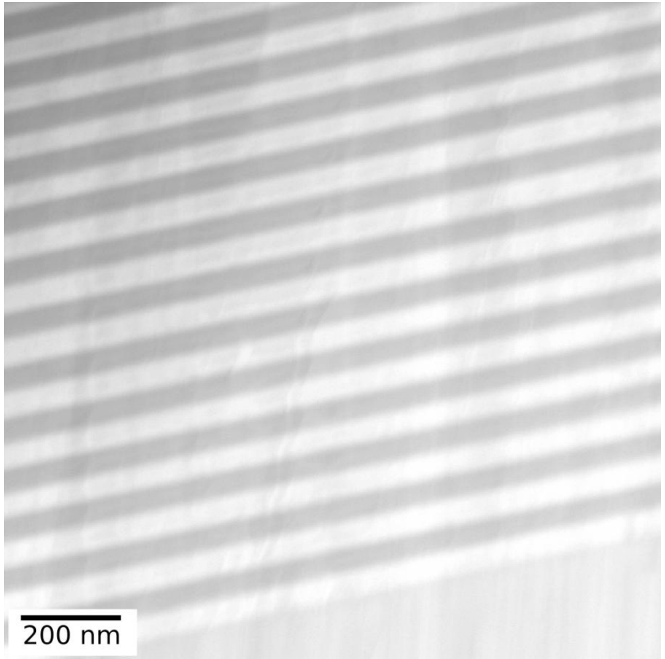

Contrast determined by atomic number

Imaging modes | Coherent vs incoherent image

Example: Si <110>

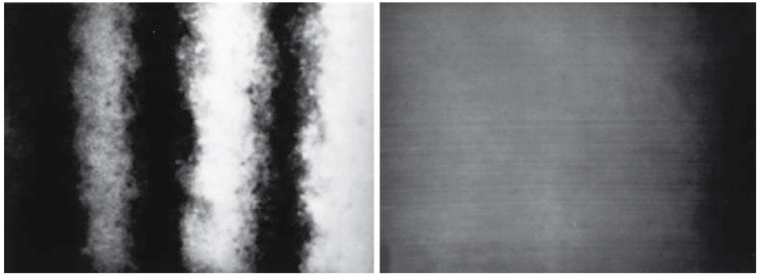

BF-STEM: Thickness fringes visible
→ Coherent

Z-contrast image
→ Incoherent

Example: Images of a Ge film grown epitaxially on Si

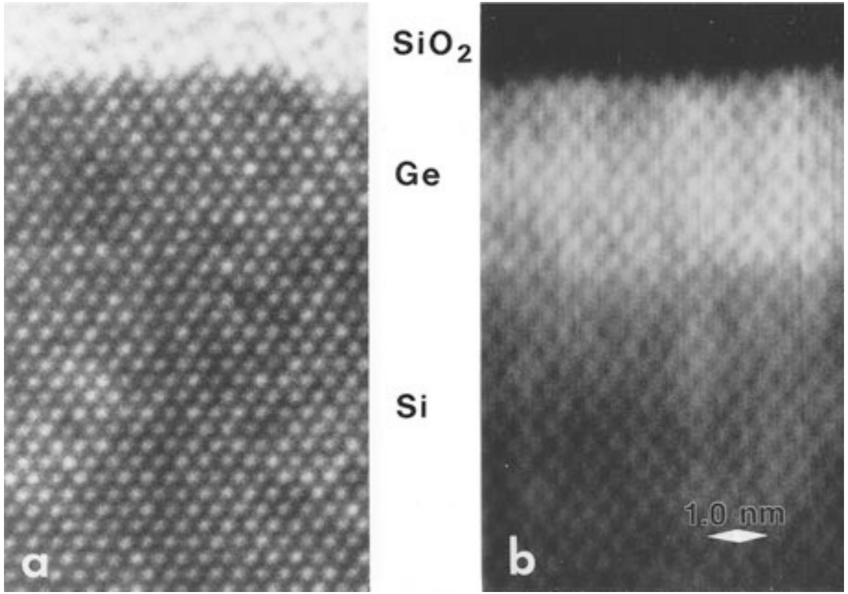

Conventional TEM image

Z-contrast image clearly delineating the Ge layer

Scattering at high angle is dependent on atomic number
No contrast reversal with focus
Images are directly interpretable: Camera cherectristic

Ultramicroscopy, 37 (1991), pp. 14-38

Imaging modes | Coherent vs incoherent image

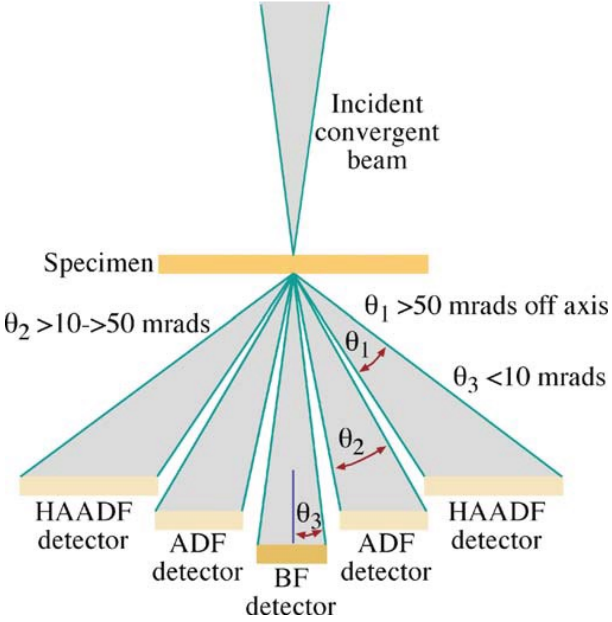

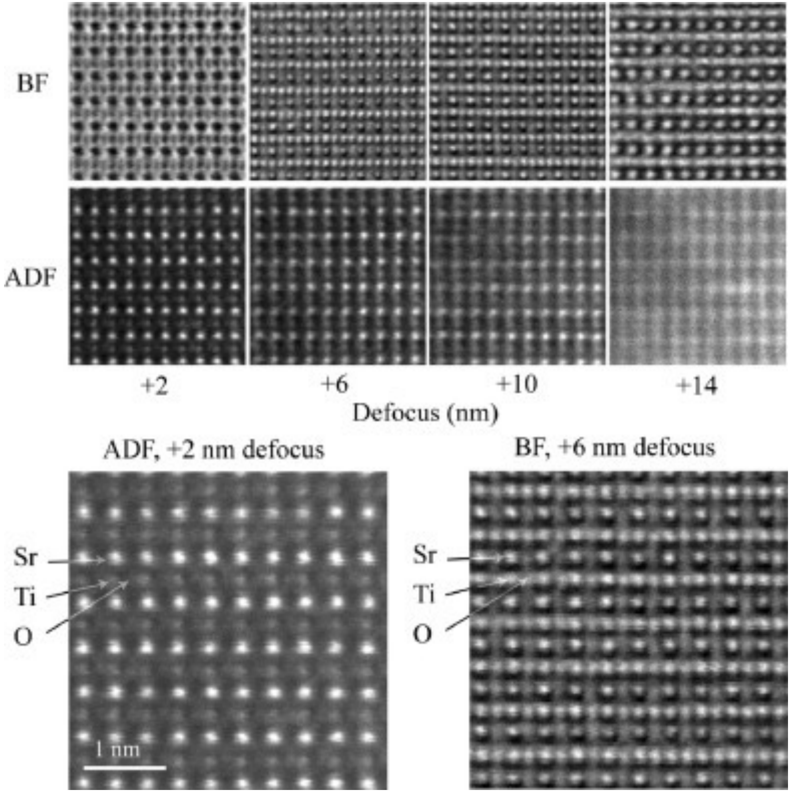

BF | On-axis → Coherent : Contrast reversal with focus/thickness

ADF | Off-axis → Incoherent (no phase relation with the inceident beam) : No Contrast reversal with focus/thickness

Pennycook S.J., Ultramicorscopy (2017) 180, 22-33.

Imaging modes | Annular bright-field

- HAADF not useful for imaging light atoms in a sample with heavy atoms because contrast so strongly dependent on atomic number.
- BF imaging has same disadvantages for imaging light atom columns similar to phase-contrast HR-TEM imaging.
- Harald Rose's annular bright-field (ABF) imaging (with aberration correction), where central part of BF detector is obscured, solves these problems.
- It is a phase-contrast image, however, because it is a sum over many point detectors, each with a different CTF; **the contrast is quite incoherent in nature over a large range of thickness and defocus**.
- Typically, the collection angle would run from half the probe angle to the full probe angle. For instance, for α = 22 mrad, use β = 11–22 mrad

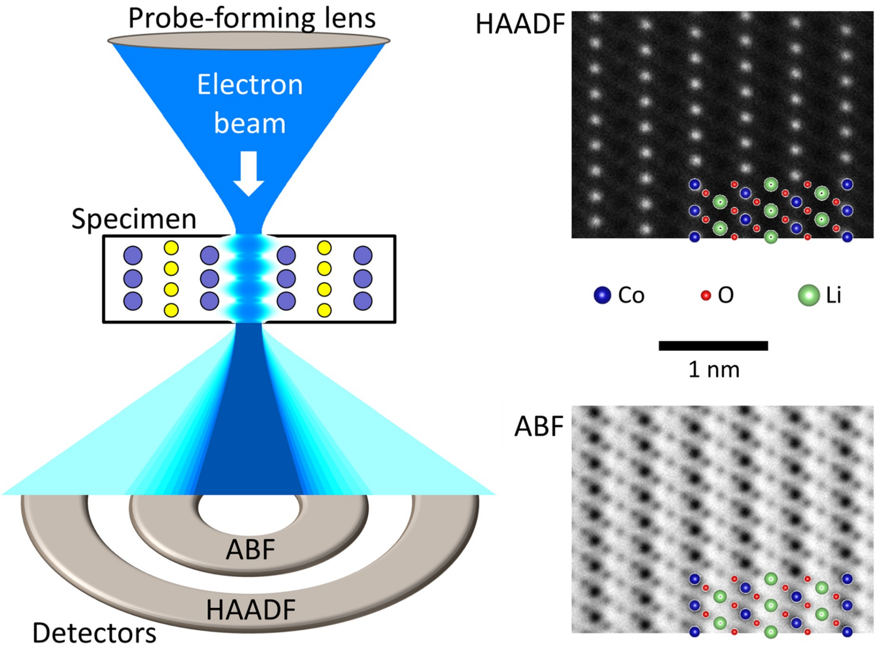

Since the ABF image is formed from low-angle scattering, it is not strongly dependent on Z, and low-Z and high-Z atoms can be seen clearly in the same image.

Findlay *et al.*, Microscopy **66** (2017).

Emad Oveisi

Imaging modes | Annular bright-field

Emad Oveisi

Simple theory: Channelled electrons scattered mostly into centre of BF detector by light columns giving some dark ABF contrast.

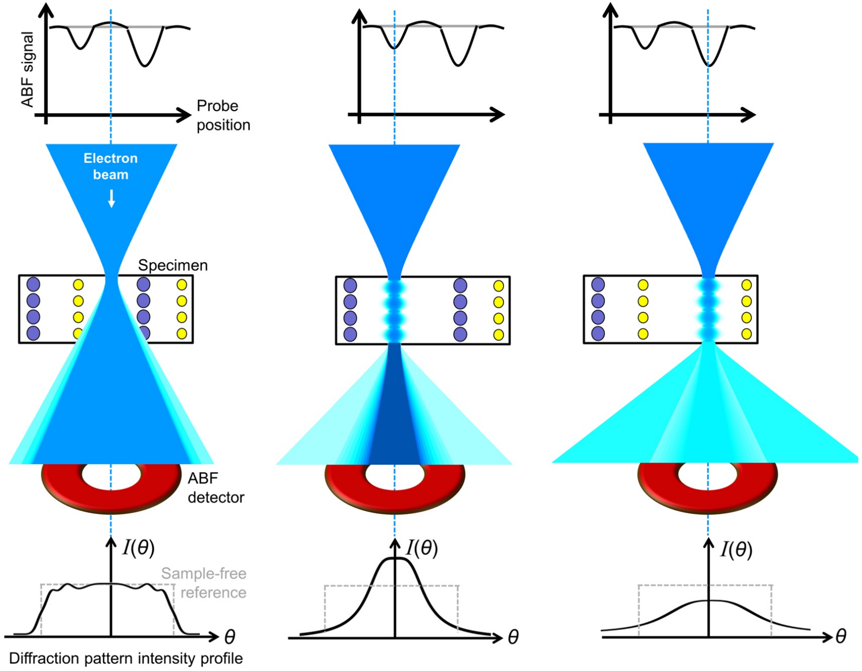

Example: $(Ba_xSr_{1-x})TiO_3$

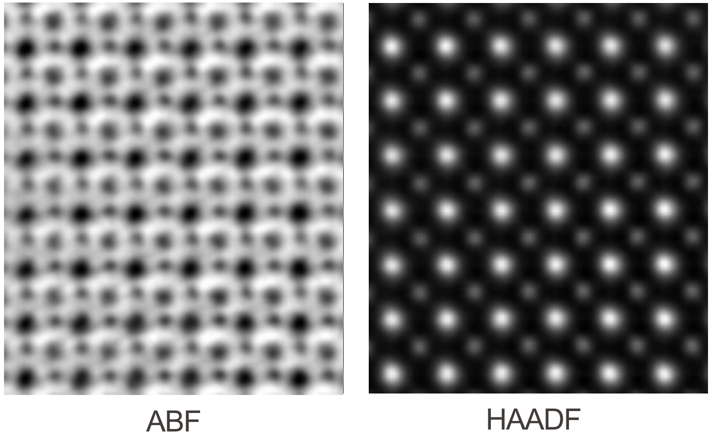

Scattered more strongly to diffracted beams by heavy columns giving darker ABF contrast. Off column little scattering, so brighter ABF contrast.

Findlay *et al.*, Microscopy **66** (2017).
Bencan and Oveisi et al. Nat. Comm. (2021).

Emad Oveisi

Shadow image | Perfect lens

Assuming perfect optics, overfocus condition

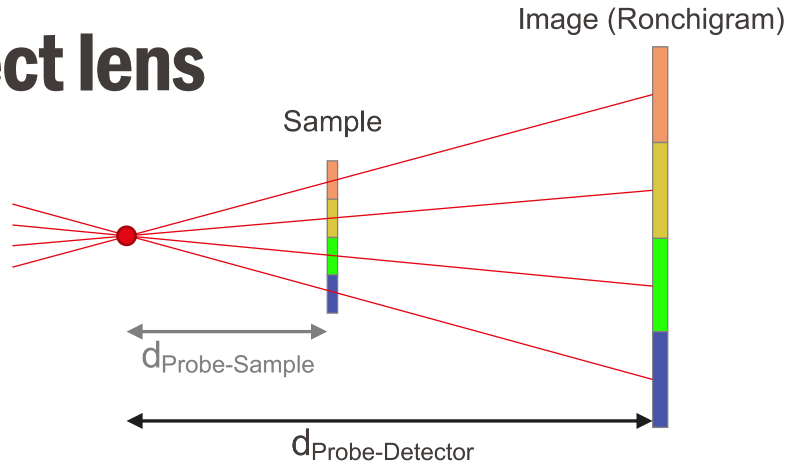

$$\text{Magnification} = \frac{d_{Probe\text{-}Detector}}{d_{Probe\text{-}Sample}}$$

At underfocus the image will magnify, but also inverted

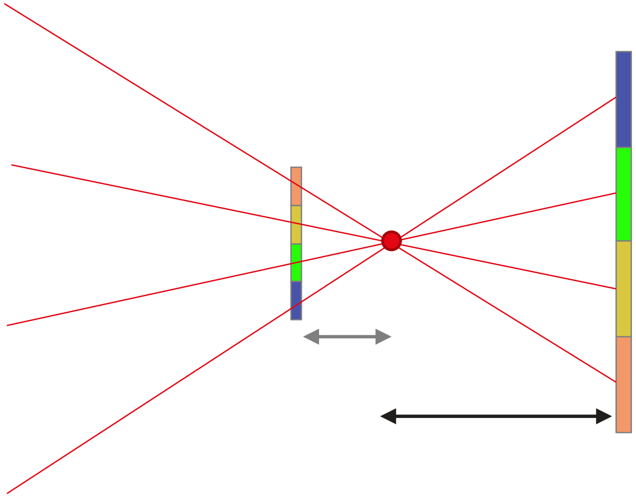

Shadow image | Real lens

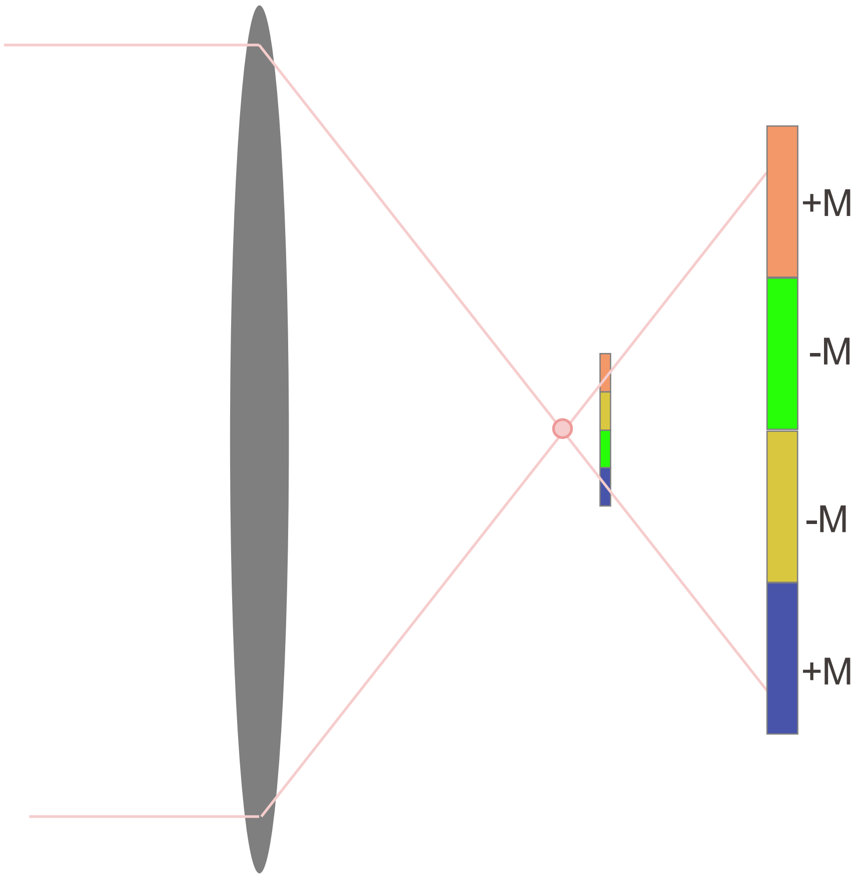

Shadow image | Real lens

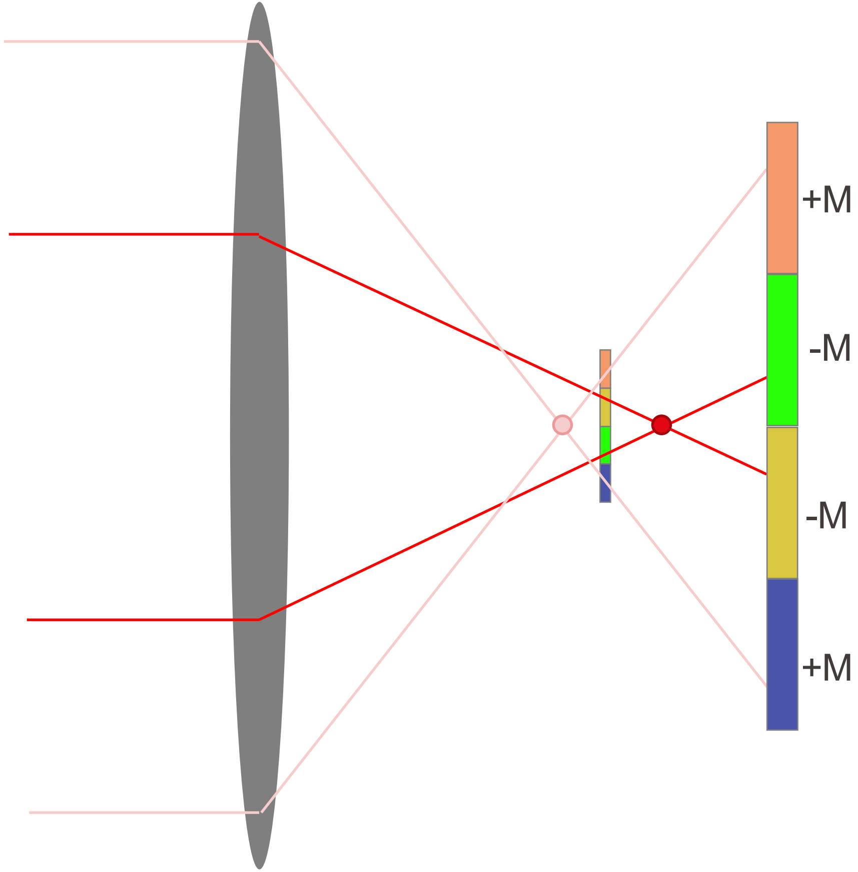

Shadow image | Real lens

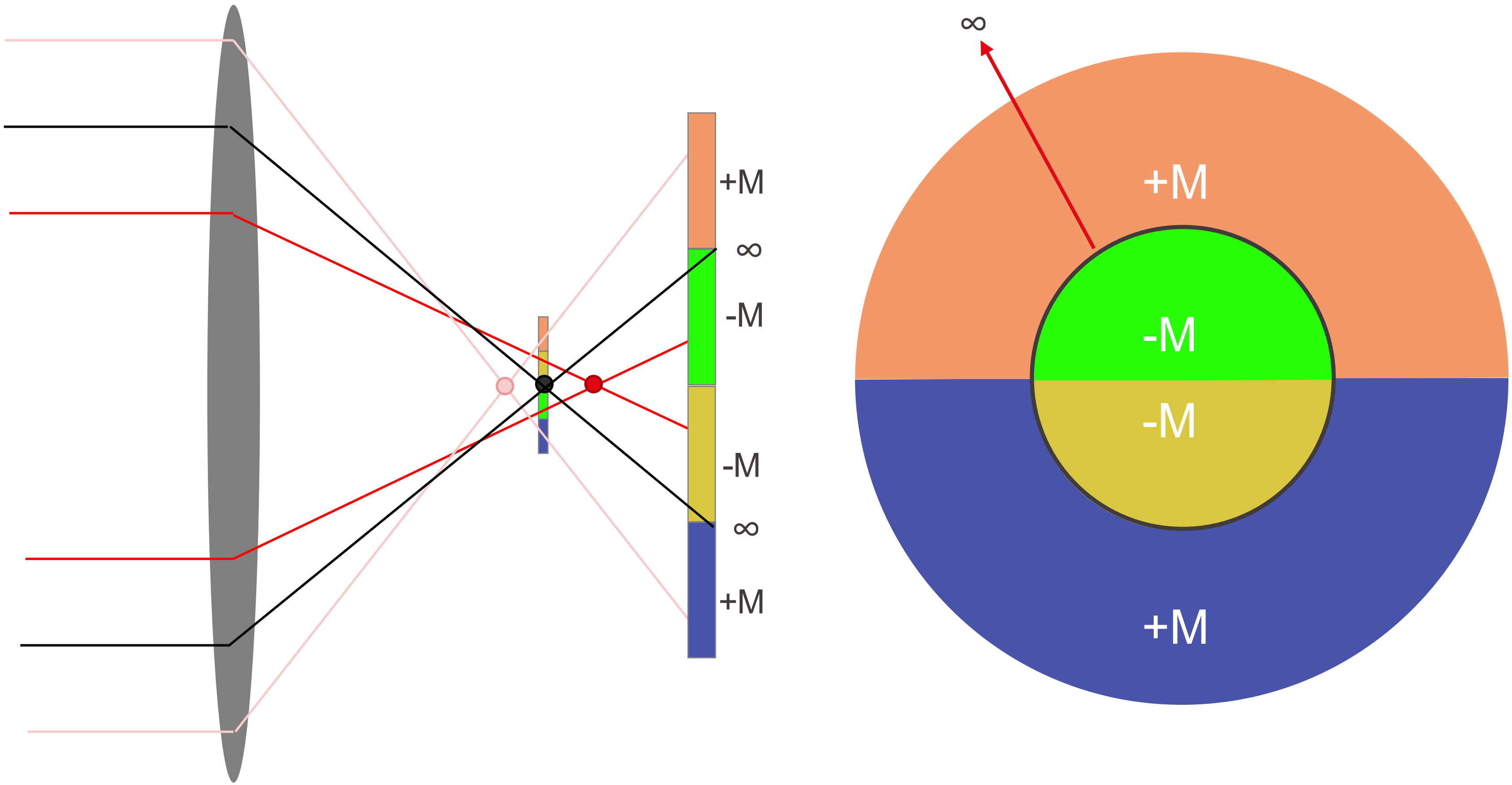

Shadow image | Real lens

In the presence of spherical aberaration, for deocus Δ and wavevektor **k,** magnifiacation M' is:

$$M' = \frac{M}{1 + C_s\lambda^2|k|^2/\Delta}$$

In 1-D infinite magnification occurs at defocus $\Delta = -\lambda^2 C_s\,|k|^2$ or $|k|^2 = \frac{-\Delta}{\lambda^2 C_s}$

In 2-D there are two critical angles for which raidal and circumferential magnifications are equal to zero:

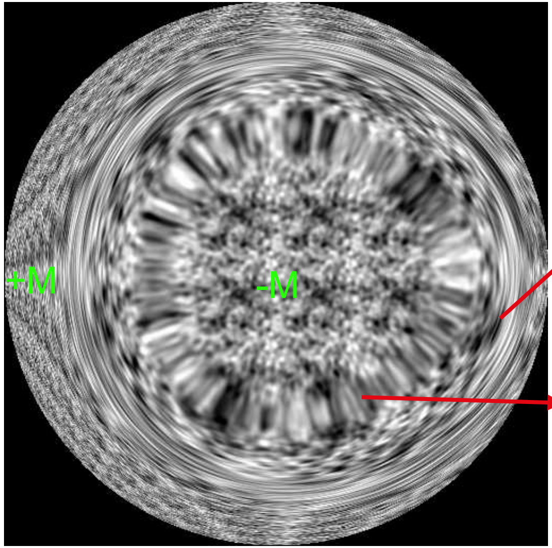

Azimuths

Radii

$|k|^2 = \frac{-\Delta}{\lambda^2 C_s}$

Circumferential

$|k|^2 = \frac{-\Delta}{3\lambda^2 C_s}$

Radial

Different Δ if there is astigmatism

The more defocus, the bigger the region in the centre which is inverted

*J.M. Cowley, Journal of Electron Microscopy Technique **3** (1986) 25.*

Emad Oveisi

Shadow image | Real lens

The more defocus, the bigger the region in the centre which is inverted

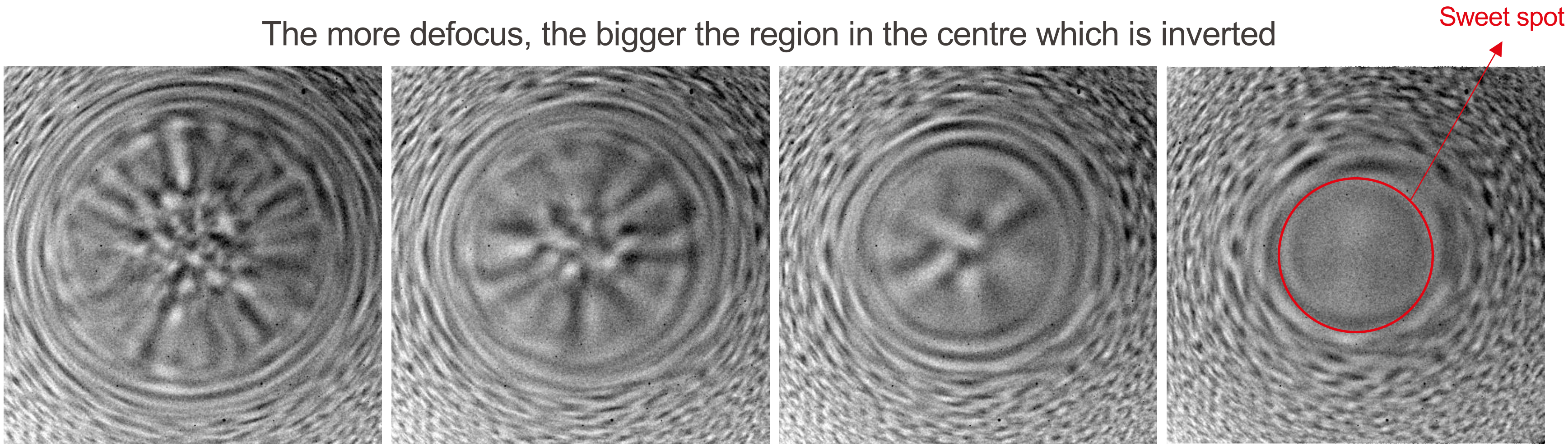

-700 nm -450 nm -250 nm Optimum defocus

In practice:

- Reduce under-focus until infinite-magnification rings are of minimum diameter
  → optimum defocus (c.f. Scherzer defocus in HR-TEM)
- Fit probe-forming aperture to the "sweet spot" region of constant phase within this

Shadow image | Resolution

STEM resolution is detemined by the size of the probe and stability of the instrument

$$\alpha_{opt} = \left(\frac{4\lambda}{C_s}\right)^{\frac{1}{4}}$$

At optimum defocus and with the correct aperture size, the probe FWHM is given by:

$$d_{opt} = 0.61\,\frac{\lambda}{\alpha_{opt}} = 0.43\,\lambda^{\frac{3}{4}}\,C_s^{\frac{1}{4}}$$

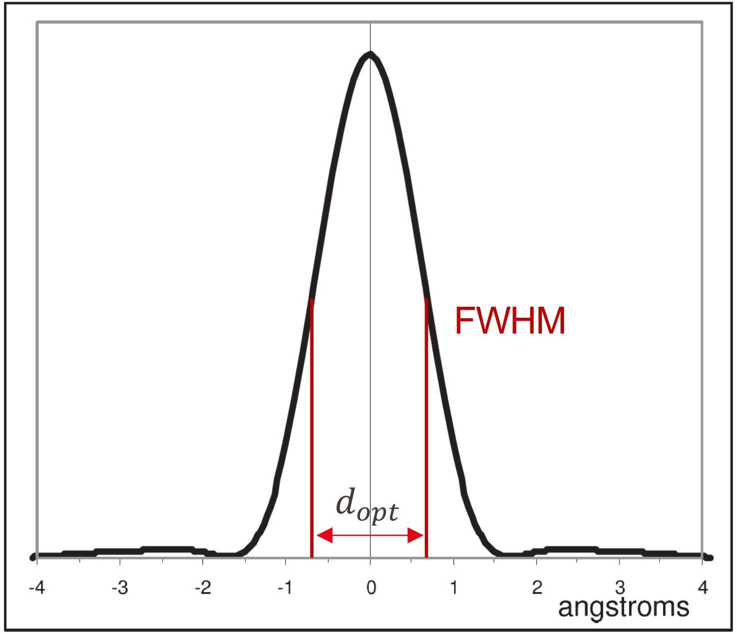

The intensity of a diffraction-limited STEM probe for the illumination conditions: Cs 1mm, and defocus z= 35.5 nm, 200kV. An objective aperture of radius 9.3 mrad has been used

Shadow image | Real lens

Different Δ if there is astigmatism → Eliptical Roncgigram instead of round

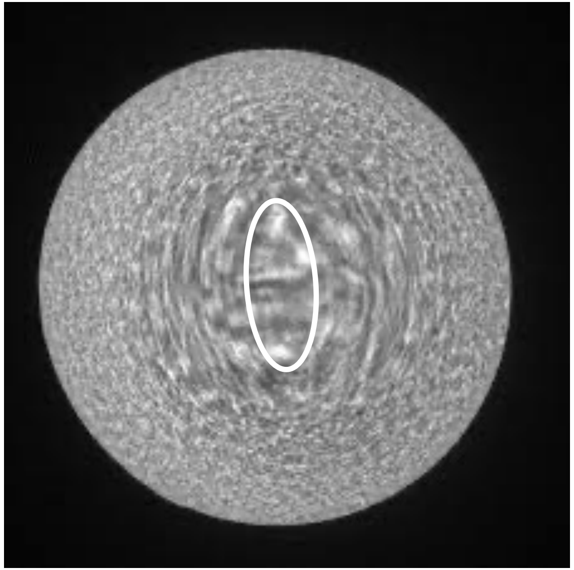

With astigmatims

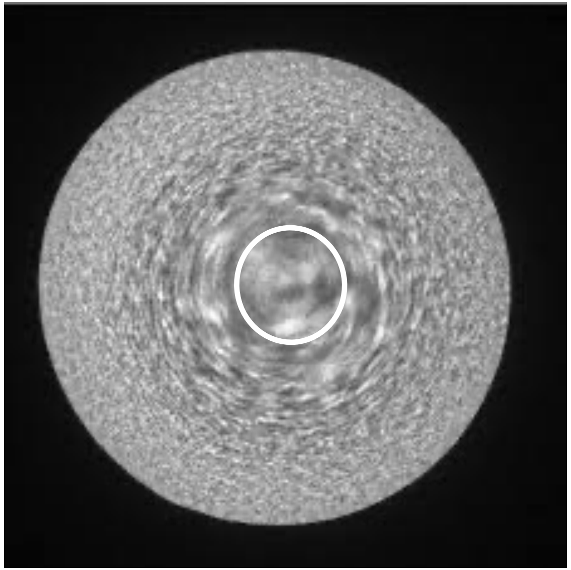

Astigmatims corrected

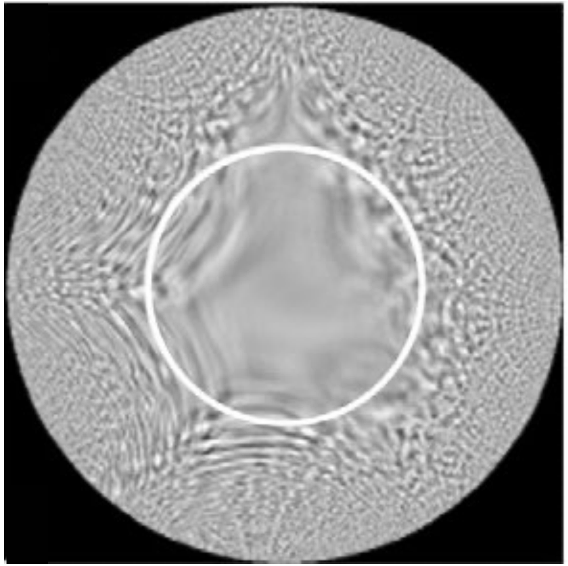

Cs corrected

Shadow image | Cs-Corrected

Emad Oveisi

Cs correction increases the size of the sweet spot

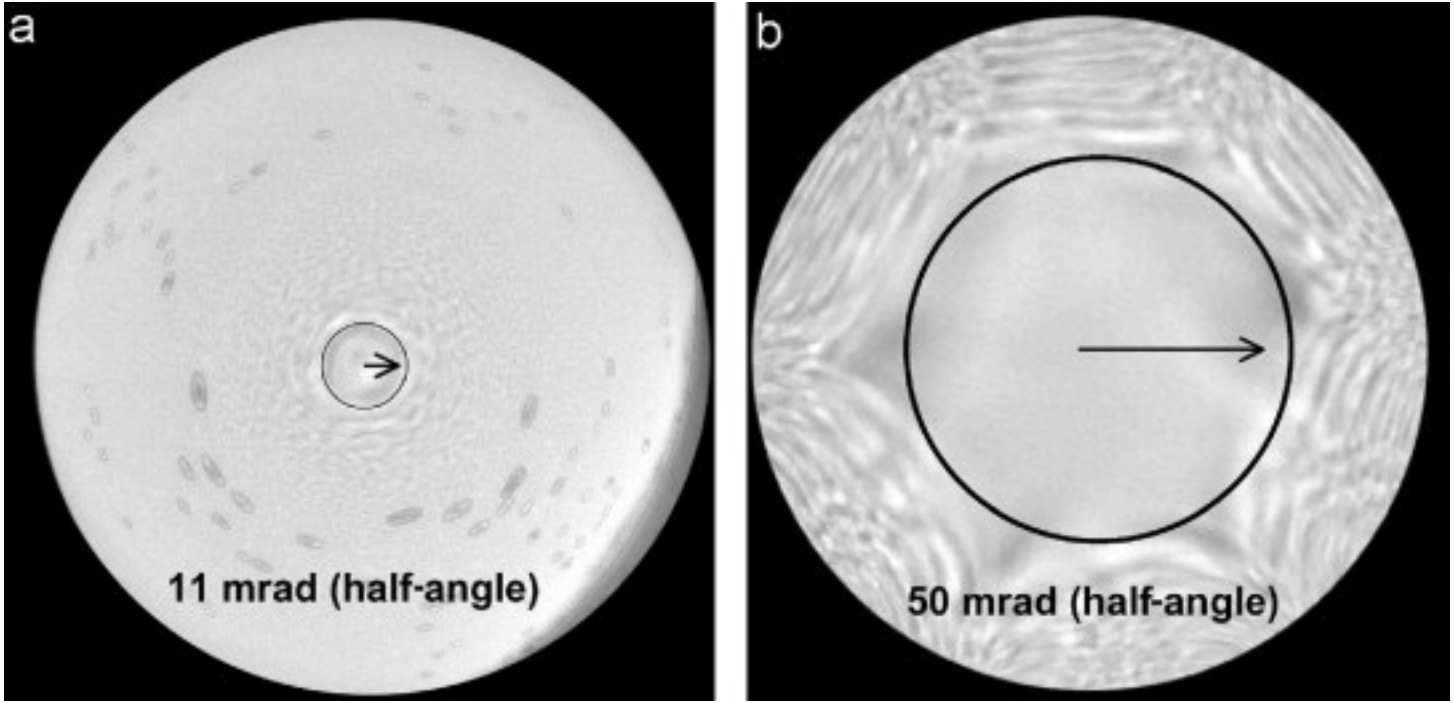

Spectrum imaging

Record spectrum as function of probe position (x, y)

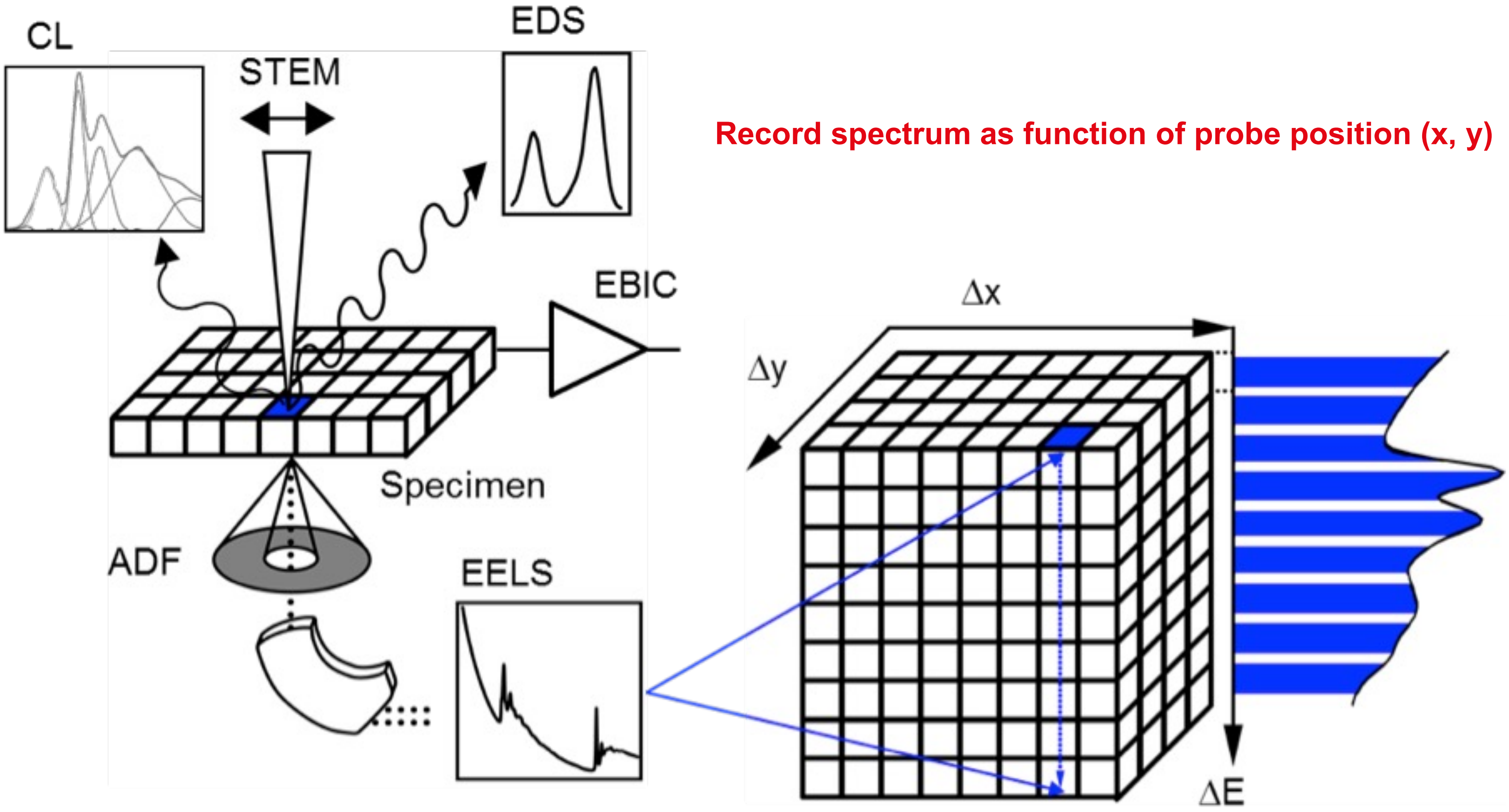

Image for Gatan.com

Energy-dispersive X-ray (EDX) STEM mapping

- High energy incident electrons (ballistic)
- → Ejection of inner shell e⁻
- Upper shell e⁻ descends
- Transition energy emitted as X-ray; characteristic of element | $E_{X\text{-ray}} = E_{Upper\ shell} - E_{Inner\ shell}$

Map X-ray intensity as function of probe position (x, y)

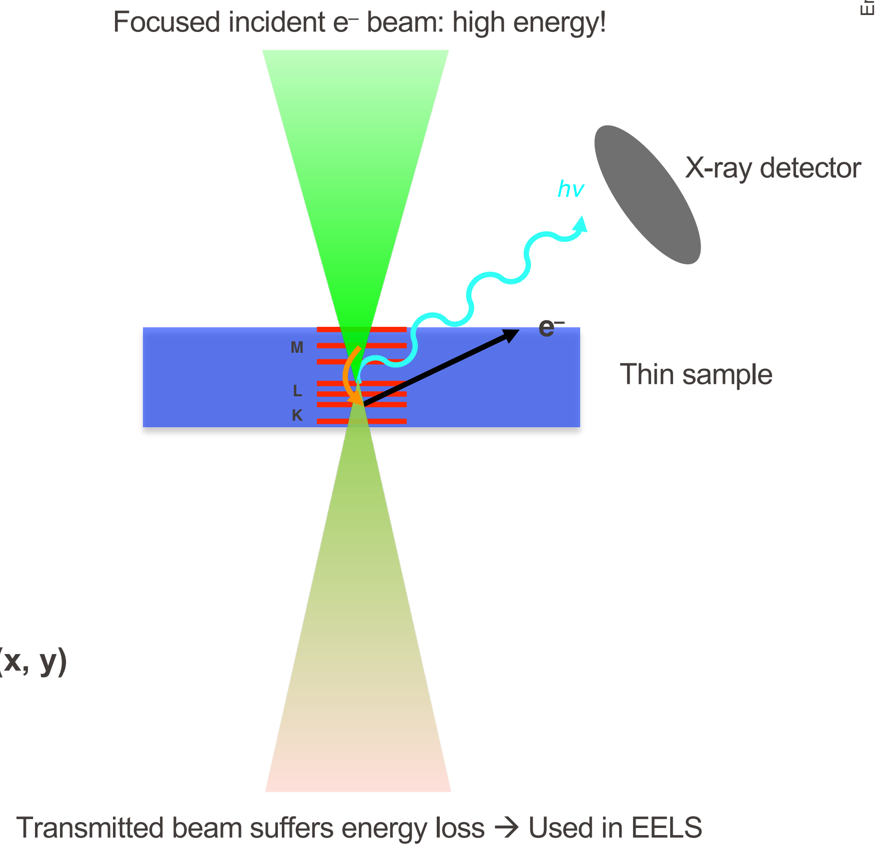

Energy-dispersive X-ray (EDX) STEM mapping

With fast mapping STEM-EDX has become a regular feedback tool for materials synthesis.

Sample characterized in a couple of minutes.

Example : Assembly of Fe_3O_4 and Cu particles

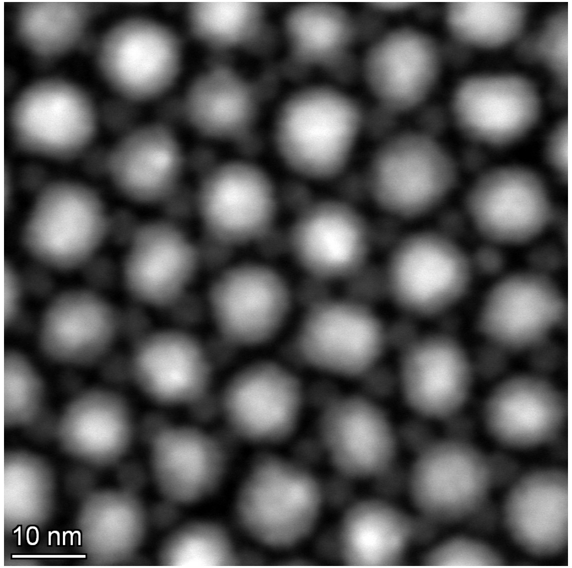

HAADF image

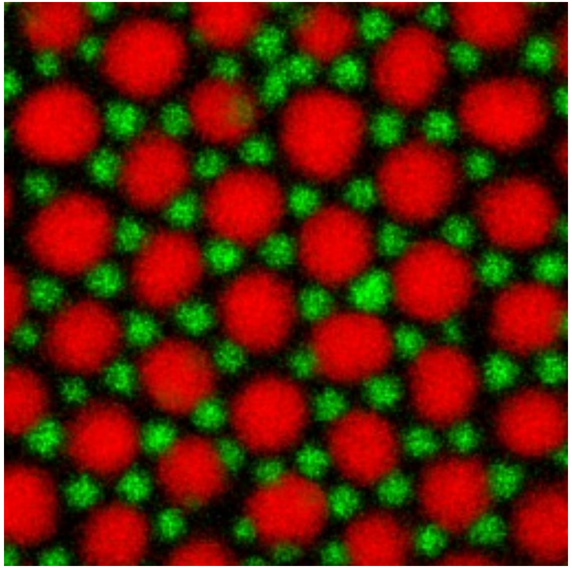

Map of Cu and Fe

In collaboration with Chethana Gadiyar LNCE, EPFL
J. Am. Chem. Soc. 2020, 142, 37, 15931–15940

Energy-dispersive X-ray (EDX) STEM mapping

With fast mapping STEM-EDX has become a regular feedback tool for materials synthesis.

Sample characterized in a couple of minutes.

Example : Ni-Rh catalytic nanoparticles in carbon shell

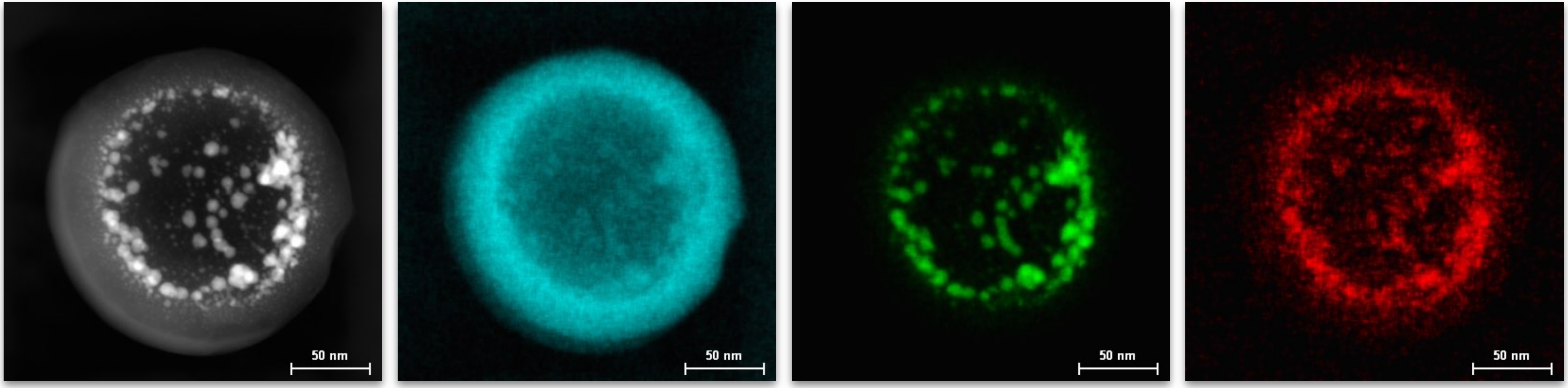

HAADF image

EDX maps of C, Rh and Ni

In collaboration with Chethana Gadiyar LNCE, EPFL

J. Am. Chem. Soc. 2020, 142, 37, 15931–15940

Energy-dispersive X-ray (EDX) STEM mapping

With aberration-corrected STEM, atomic resolution EDX became possible

Example: $(Ba_xSr_{1-x})TiO_3$

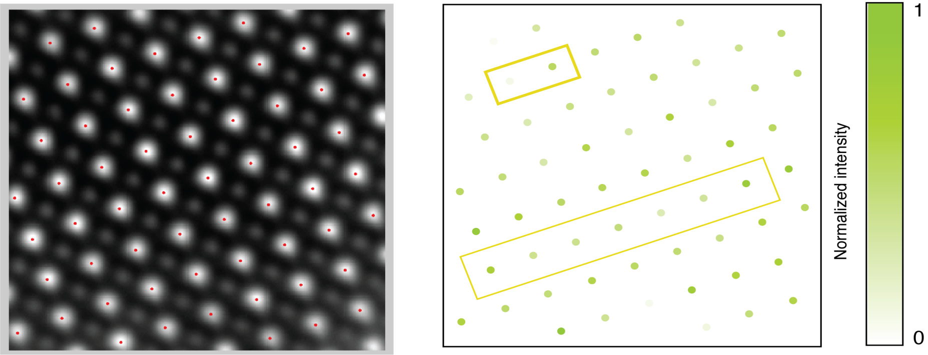

HAADF image

Intesnsity map

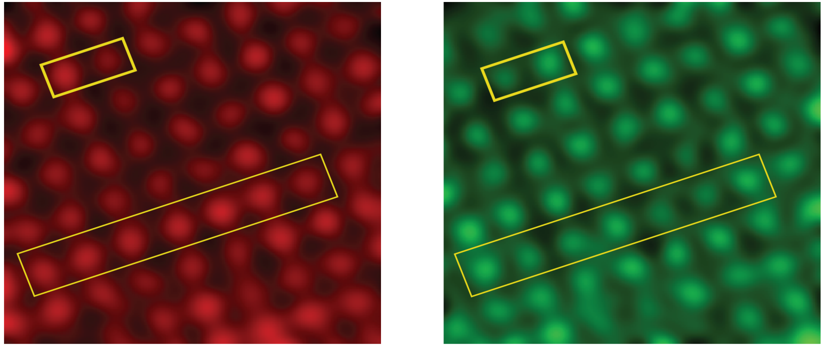

EDX maps of Sr and Ba

In collaboration with Prof. Dragan Damjanovic, EPFL
Bencan and Oveisi *et al.* Nature Communications 2021.

Electron energy-loss spectroscopy (EELS)

The TEM specific microanalysis technique!

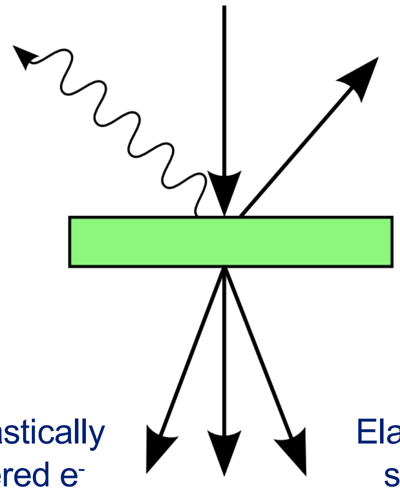

More details in Duncan Alexander's EELS lecture this afternoon

Principle of energy-loss spectrometry

Incident electron beam with energy E_0

Inelastic scattering of electrons in specimen; energy loss ΔE

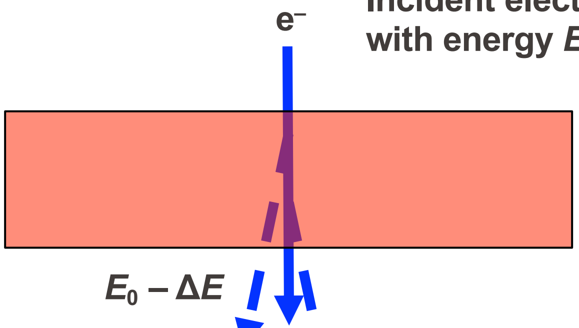

Magnetic prism separates electrons with different energy; produces spectrum of intensity J(E) vs energy loss ΔE
– *the energy-loss spectrum*

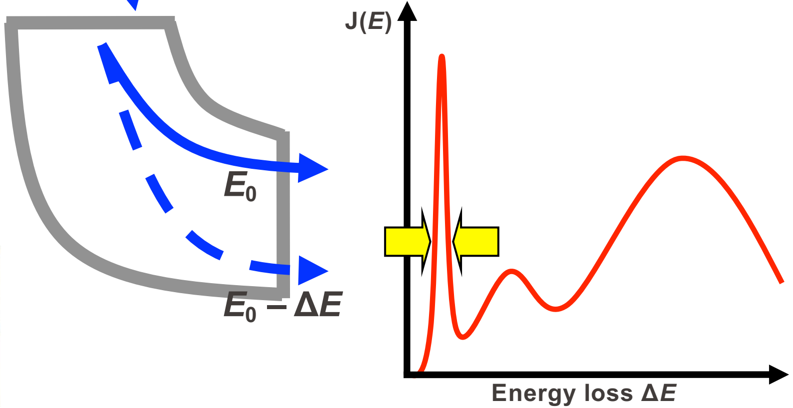

e.g. Gatan Enfina

Emad Oveisi

The EELS spectrum | Zero loss

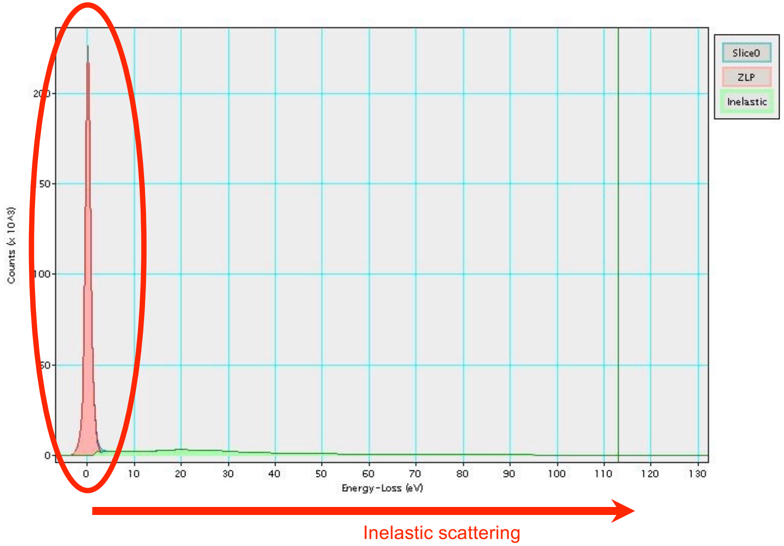

Zero-loss: Elastically-scattered e^-

Information about speciemen thickness

The EELS spectrum | Low-loss

Interaction with outer electrons (conduction/valence)

Low-loss spectrum 0-50 eV: valence excitations - plasmons (bulk & surface), band gaps, optical properties

The EELS spectrum | Core-loss

Emad Oveisi

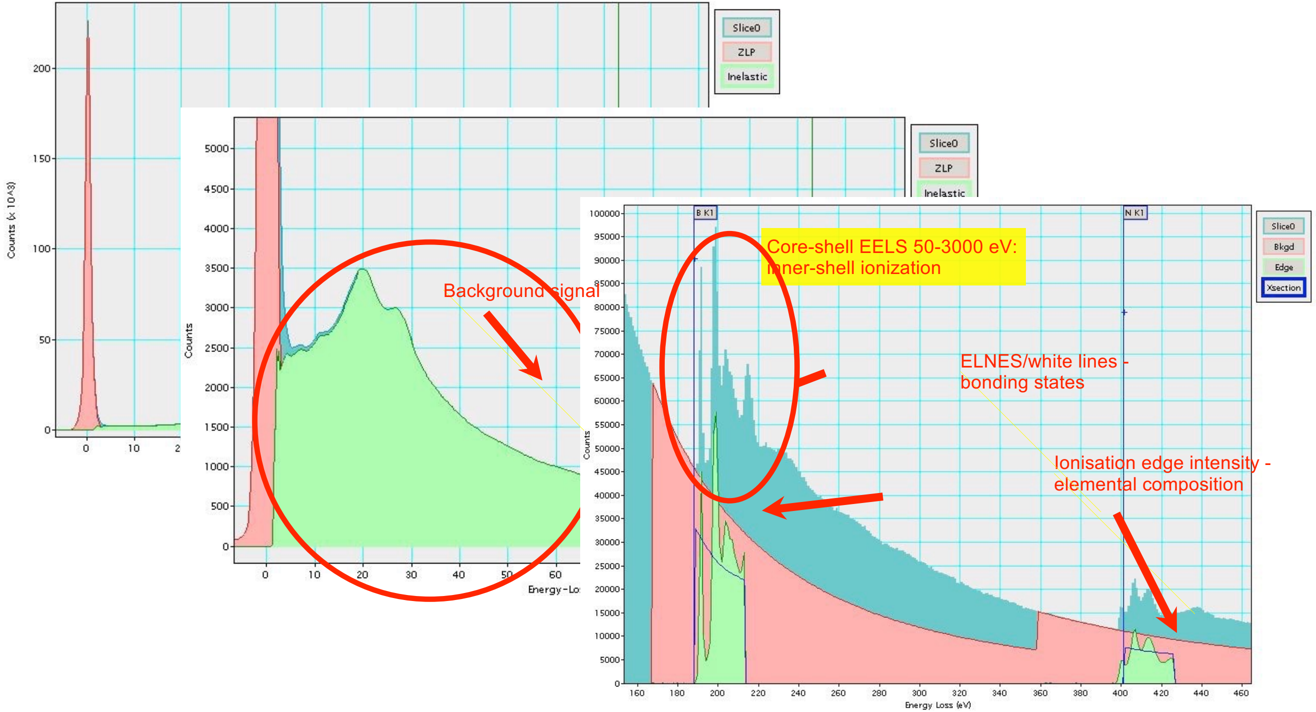

Interaction with core electrons

Core-loss spectrum 50-3000 eV: inner shell ionization

ELNES/white lines: Bonding state

Ionisation edge intensity: elemental composition

Atomic resolution core-loss STEM-EELS

Example: Atomic resolution spectroscopic imaging of a $La_{0.7}Sr_{0.3}MnO_3$ / $SrTiO_3$ multilayer, showing the different chemical sublattices in a 64 × 64 pixel spectrum image extracted from 650 eV–wide electron energy-loss spectra recorded at each pixel.

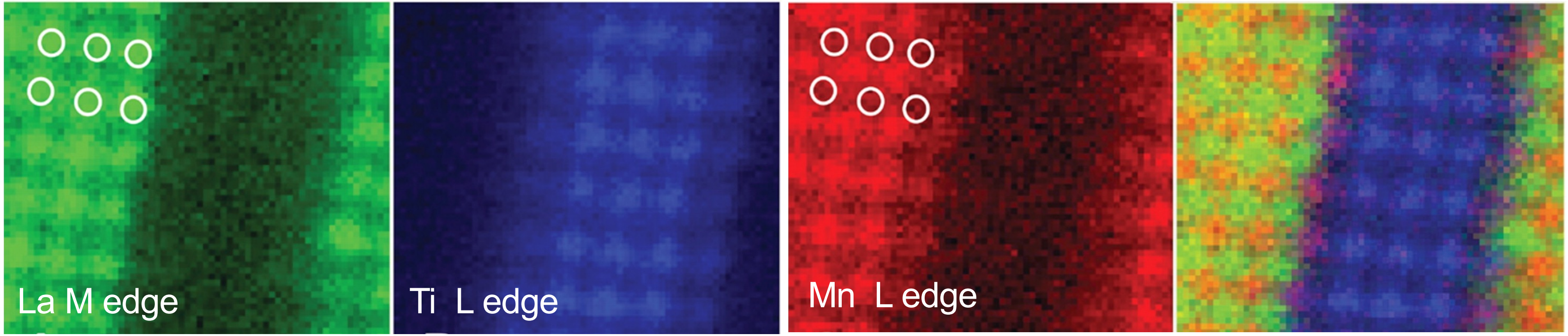

D.A Muller *et al.*, Science 2008.

Emad Oveisi

Sample quality and imaging concerns

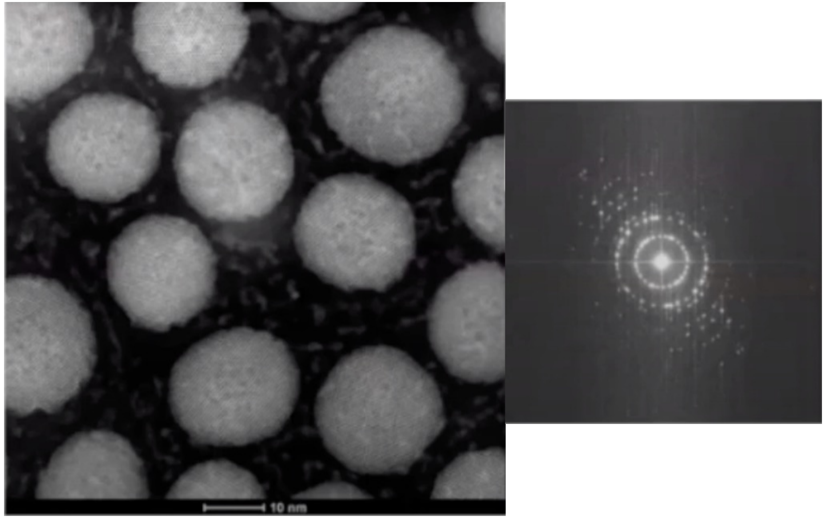

Without sample drift

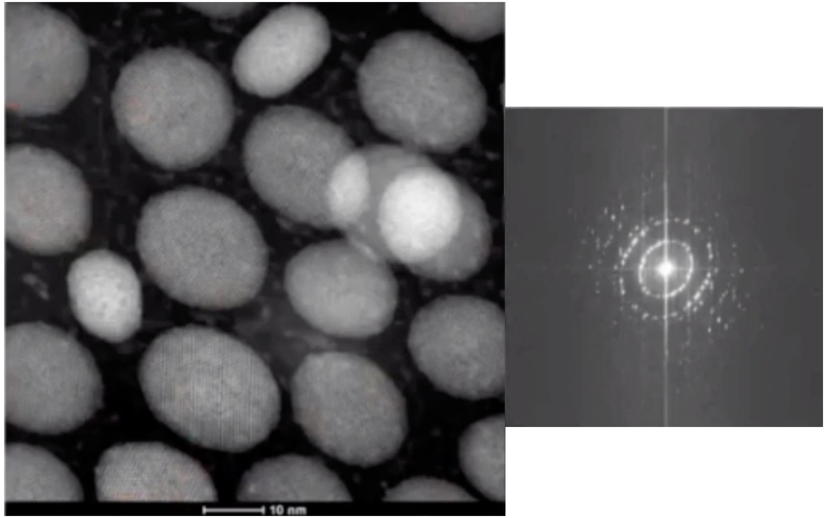

With sample drift

Sample quality and imaging concerns

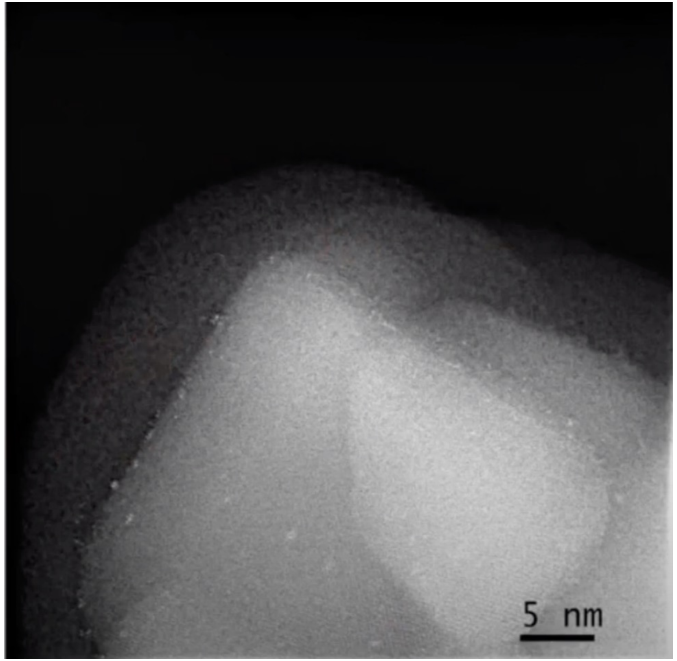

Beam induced contamination

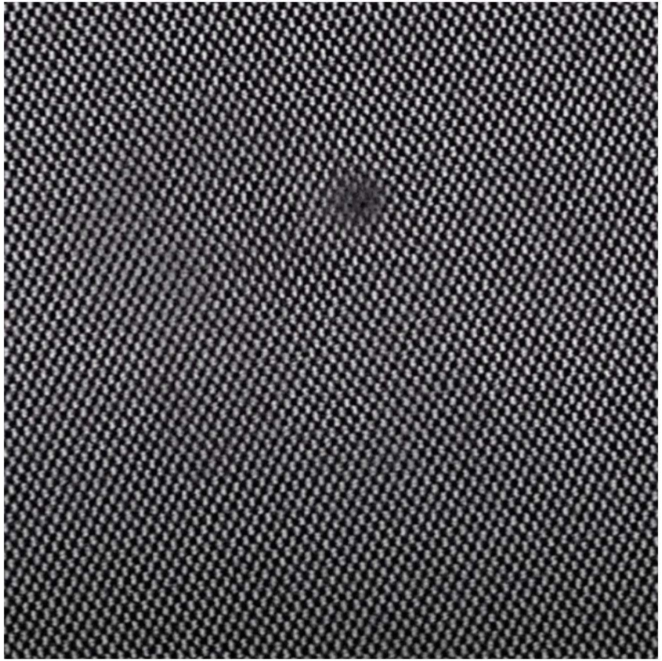

Beam induced damage (hole)

Sample quality and imaging concerns

Represenatative of sample

Thin

Stabe under vaccum and probe current

Free of contamination

Uniform thickness

Conductive

Summary

Aberration-correction and improved instrument stability give sub-Å resolution in STEM.

With lower beam voltages lighter elements can be analyzed without beam damage.

Faster, more sensitive spectrometers give unprecedented access to composition, chemistry and physics of materials.

Computer interfaces and software allow acquisition and processing of large datasets.

STEM is now not one technique that can be easily summarized, but is split into many specialisms.

Many other possible uses (e.g. imaging of magnetic domains, optical plasmon mapping, *in situ* studies) exist. The new equipment at CIME cover the majority of these possibilities, creating a state-of-the-art facility at EPFL.

With the latest instrumentation, the sample and specimen preparation are often the limiting factor!

Some useful literature

Scanning Transmission Electron Microscopy by S.J. Pennycook and P.D. Nellist (eds) (Springer)

Aberration-corrected imaging in transmission electron microscopy: an introduction by R. Erni

Transmission Electron Microscopy by D.B. Williams and C.B. Carter (Springer)

Large Angle Convergent Beam Electron Diffraction by J.-P. Morniroli

Transmission Electron Microscopy and Diffractometry of Materials, Fultz and Howe

Science of Microscopy by C.W. Hawkes and J.C.H. Spence (eds) (Springer)